

THE McMASTER POLARIZED ION SOURCE

THE McMASTER POLARIZED ION SOURCE

By

JOHN WALLACE McKAY, B.Sc.

A Thesis

Submitted to the School of Graduate Studies
in Partial Fulfilment of the Requirements

For the Degree

Master of Science

McMaster University

April 1976

MASTER OF SCIENCE (1976)
(Physics)

McMaster University,
Hamilton, Ontario

TITLE: The McMaster Polarized Ion Source

AUTHOR: John Wallace McKay, B.Sc.
(University of Toronto)

SUPERVISOR: Professor John A. Kuehner

NUMBER OF PAGES: v,59

SCOPE AND CONTENTS:

The theory of the Lamb-Shift, Spin-Filter polarized ion source is discussed. The design and construction of such a source for the McMaster University Tandem Accelerator is described. Finally, measurements and calibrations of the operating parameters are presented.

ACKNOWLEDGEMENTS

I would like to thank Doctors John Kuehner, Robert Summers-Gill, and James Waddington for their help and patience during the years of this project. I would also like to mention with gratitude, the invaluable assistance received from Dr. J.L. McKibben and his co-workers at the Los Alamos Scientific Laboratories

TABLE OF CONTENTS

	<u>Page</u>
DESCRIPTIVE NOTE	ii
ACKNOWLEDGEMENTS	iii
TABLE OF CONTENTS	iv
INTRODUCTION	1
CHAPTER I GENERAL DESCRIPTION OF THE SOURCE	4
CHAPTER II THEORY OF OPERATION	10
CHAPTER III OPERATIONAL PROCEDURES	36
CHAPTER IV CALIBRATION OF SOURCE PARAMETERS	48
CHAPTER V CONCLUSION	56
REFERENCES	58

LIST OF FIGURES

	<u>Page</u>
Figure 1 The McMaster Polarized Ion Source	7
Figure 2 Polarized Ion Source Schematic	8
Figure 3 Location of Source	9
Figure 4 Hydrogen Breit-Rabi Diagram	15
Figure 5 Deuterium Breit-Rabi Diagram	16
Figure 6 Spin Filter Fields	18
Figure 7 The Lamb Shift	19
Figure 8 Spin State Polarization	34
Figure 9 Block Diagram of the R.F. System	42
Figure 10 Argon Flow & Caesium Temperature Data	50
Figure 11 Comparison of Krypton and Argon Adder Gas	52
Figure 12 Argon Coil Shunt Settings	53
Figure 13 Precursor Calibration	55

INTRODUCTION:

The use of polarized ion beams in the investigation of nuclear structure physics, has been increasingly recognized in recent years as a powerful technique. In 1971, it was decided that a polarized ion source should be added to the facilities at the McMaster University Tandem Accelerator Laboratory. The initial impetus for this, was to exploit two new and potentially powerful techniques for the study of nuclear structure. The first is a model independent method for determining the parity of a nuclear level as either $\pi=(-)^J$ or $\pi=(-)^{J+1}$ and for the unique identification of 0^- levels. (1) The second method uses (\vec{d}, α) angular correlation measurements in odd-odd nuclei. (2)

The parity determination technique utilizes the fact that, for 100% tensor polarized deuterons ($t_{20}=-\sqrt{2}$) with the quantization axis aligned to the beam direction, and incident on a spin zero target, the (\vec{d}, α) reaction can have yield at 0° or at 180° only for levels which have unnatural parity ($\pi=(-)^{J+1}$). It can also be shown that the yield ratio (tensor polarized beam:unpolarized beam) must be $(1 + t_{20}/\sqrt{2})$ for natural parity and $(1 - \sqrt{2} t_{20})$ for 0^- levels. The second technique extends the "Litherland-Ferguson method II" (using spin zero reactions with particle-gamma ray angular correlation measurements to make spin assignments in even-even nuclei) to odd-odd nuclei. This experiment requires a (relatively) intense beam of tensor polarized deuterons.

There were about seventeen major polarized ion sources in the world when this project was started. ⁽³⁾ Either the Los Alamos device or a more recent version of this design at the Tri University Nuclear Laboratory appeared to be quite capable of producing the desired beam. These two sources are unique in that they employ the "Lamb Shift-Spin Filter" method to produce a polarized beam. Only this method is capable of producing intense tensor polarized beams with a high degree of polarization.

The field of polarized ion production has been the subject of active research for more than twenty years. A number of review articles have been published, for example, by England, ⁽⁴⁾ Glavish, ⁽⁵⁾ and Clegg. ⁽⁶⁾ Two very different approaches have been developed and refined over the years; the "Atomic Beam" technique, and the "Lamb Shift" technique.

In an Atomic Beam device, neutral hydrogen atoms are aligned and the substates are spatially separated by a multipole magnet. The concept is an elaboration of the classic Stern-Gerlach experiment.

The "Lamb Shift" devices utilize metastable $n=2$ hydrogen in a magnetic field (~575 gauss). Quenching of $2S_{1/2}, m_J = -1/2$ substates can be induced because they and the $2P_{1/2}, m_J = +1/2$ levels are degenerate at that field. Polarization is then achieved by field reversal (Sona method ⁽⁷⁾), or by the use of the 3 level interaction "Spin Filter".

In June 1972, funding arrangements were made and a contract was let to General Ionex Corporation (Ipswich Mass., U.S.A.) for the detailed design and assembly of the main source deck and its controls. Beam

precession and injection hardware as well as many of the main deck components were constructed by McMaster University. The Los Alamos group acted as consultants for this project. Construction was completed in late June 1974 and preliminary testing was begun. By mid July, the usual vacuum and assembly problems had been solved. A 100 nA negative beam was observed briefly before the source was disassembled and shipped to McMaster. The first polarized beam was produced on December 4, 1974, and the first polarized beam on target was achieved February 18, 1975. In the following year, over 20% of scheduled beam time on the FN accelerator has been for the use of polarized ions. A large number of papers and presentations have resulted from this first year's work. (1,2,8)

This thesis will describe the theory of operation of the source, its design and construction. Some operational considerations will be discussed, and calibration measurements will be presented.

CHAPTER I
GENERAL DESCRIPTION OF THE SOURCE

This ion source is a large and complex unit. Many thousands of hours of work had gone into development of this design at the Los Alamos Scientific Laboratories before the McMaster project began. Detailed information on all aspects of the source construction and operation was made readily available to us by the L.A.S.L. personnel. The McMaster source is therefore, a development of the L.A.S.L. design incorporating a number of improvements suggested by their experience.

This section of the thesis will identify and briefly describe the functional divisions and components of the source. The source components are shown in figure 1 and the functional divisions in figure 2.

The first function is the production of a high intensity beam of positive ions (protons or deuterons). This is done with a conventional Von Ardenne duoplasmatron with an expanded plasma extraction cup. An arc current of up to 17 amps is used. This is a high power level for a nuclear physics ion source. For example, the regular ion source on the McMaster FN tandem runs with an arc current of about 1 to 3 amps. The beam is extracted at about 7 kilovolts then decelerated to 500 eV for proton beams, or 1000 eV for deuteron beams. This is necessary for the resonant charge exchange processes that follow.

The positive beam enters a caesium vapour canal next, where metastable H(2S) neutrals are produced with an efficiency of about 30%. The presence of caesium vapour also provides space charge cancellation

in the ion beam. This is necessary to prevent expansion of the positive beam. A large number of ground state neutral atoms and charged ions are also produced in the canal. These must be eliminated or they will degrade the polarization of the final beam.

The spin filter region is located in a uniform axial magnetic field where appropriate electric fields generate multi level interaction. The required fields are a 1.6 GHz. longitudinal field, and a small (~15 volts/cm) transverse DC field. The latter also serves to deflect the charged ion beam. These spin filter fields selectively quench all but a single m_I substate to the ground state.

The neutral beam of polarized metastables and the unpolarized ground state atoms now enter the Argon canal. A small axial magnetic field in this region determines the final polarization of the beam as the negative ions are formed. At the ion velocities used, the metastable atoms are preferentially negatively ionized compared to the ground state atoms. The ionized polarized beam is then separated from the unpolarized ground state neutral beam. The large flow of Argon used in the process is pumped by two helium cryostats located, one at each end of the canal. They operate at about 20°K.

The negative beam is next accelerated through a three gap lens to injection energy, usually 70 keV.

The optical elements of the injection line are two einzel lenses, two weak electrostatic quadrupole lenses and a 15° inflection magnet. A "Wien Filter" (crossed magnetic and electric fields) precesses the polarization axis to the direction required for the experiment.

The ion source components sit on a large insulated deck about two meters long. This deck contains all the pumping and cooling equipment. An adjacent deck of four standard sized electronics racks, contains the power supplies and controls. All this is located within a protective grounded cage. A concrete shielding wall between the source and the accelerator protects the operator from radiation. Figure 3 shows the layout of the source and the injection line.

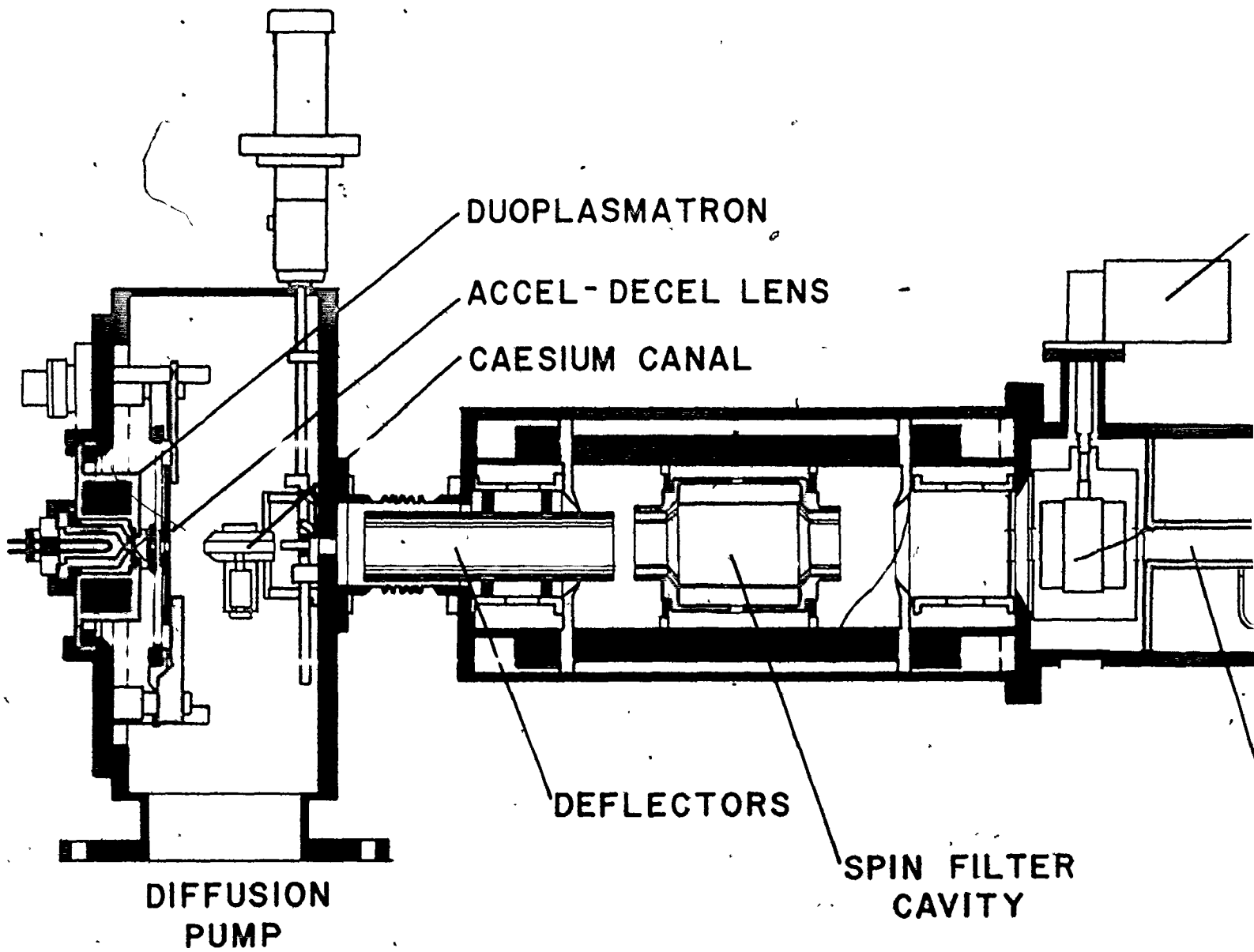


figure 1

THE M^CMASTER POLARIZED

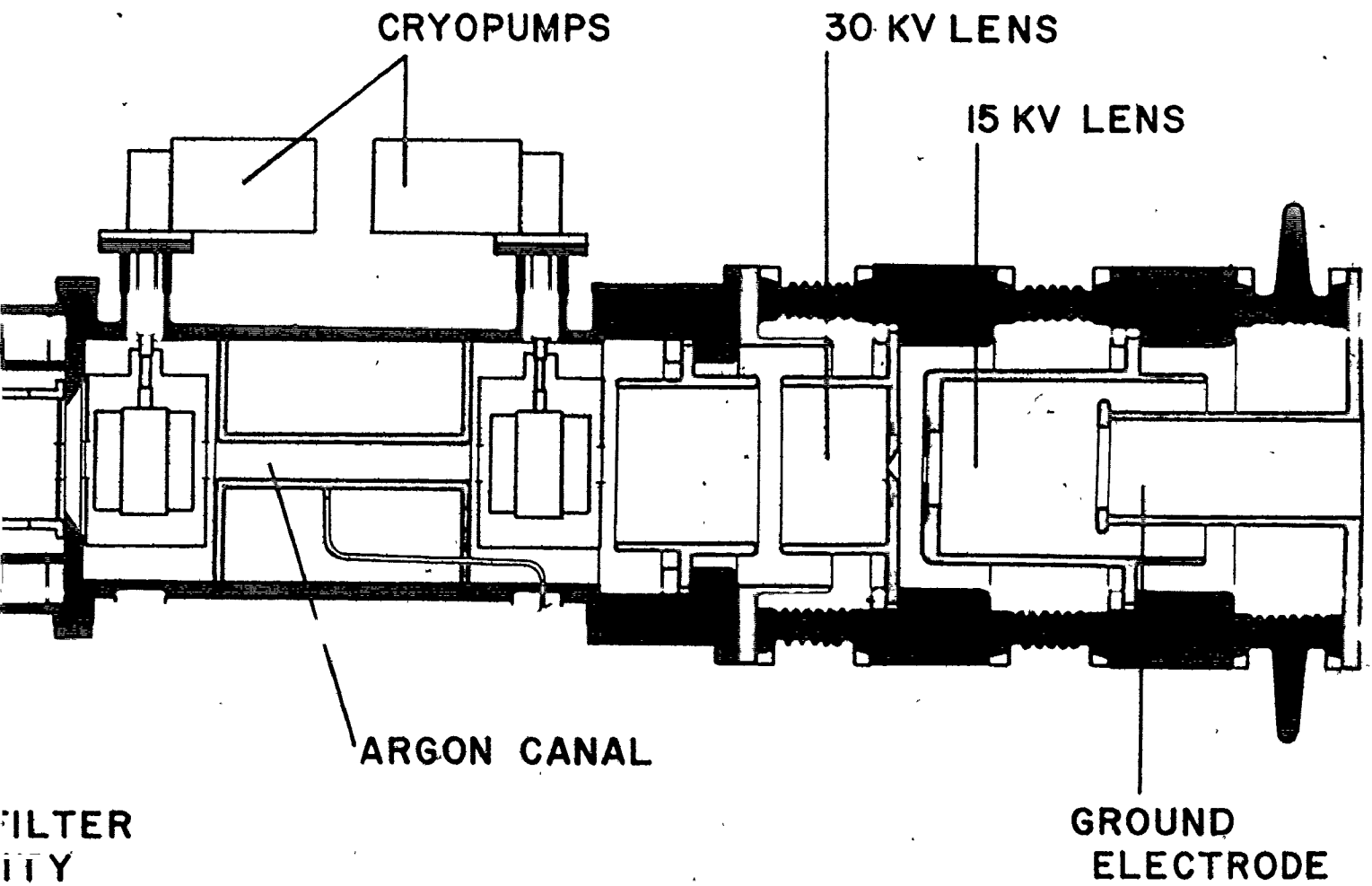


figure 1
POLARIZED ION SOURCE

POLARIZED ION SOURCE SCHEMATIC

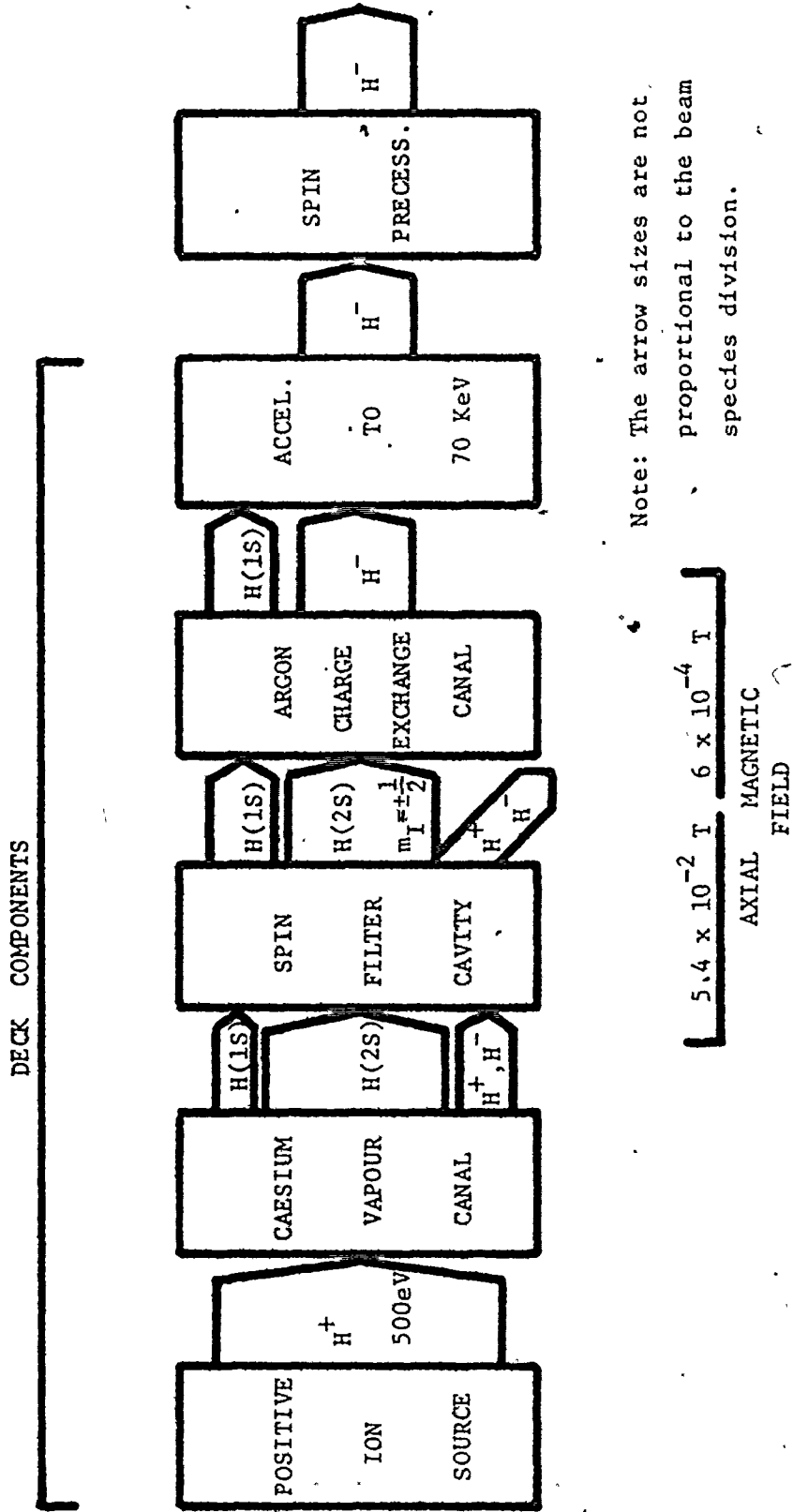


FIGURE 2

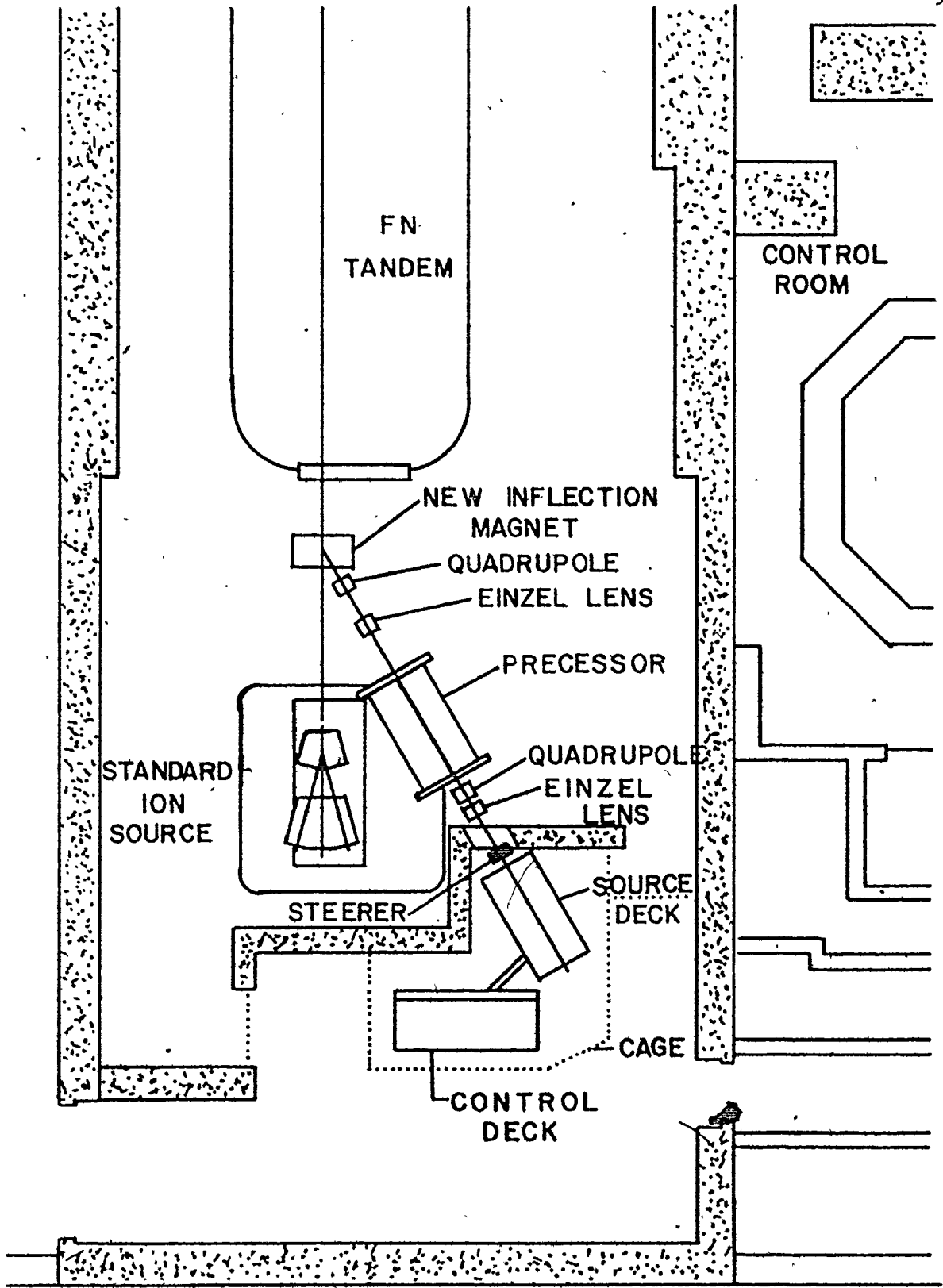


FIGURE 3 LOCATION OF SOURCE

CHAPTER II
THEORY OF OPERATION

The Positive Beam System:

The duoplasmatron source invented by Von Ardenne, has for years been the work horse of ion sources. The polarized ion source uses a standard design of duoplasmatron running at up to 17 amps of arc current. While this unit is high powered by tandem accelerator standards, it must be kept in mind that duoplasmatrons of up to 3000 amperes, peak arc current are used in fusion research. The filament is a hairpin shape rolled out of nickel mesh coated with a low work function emission compound. This will last through a typical several day run. Once an arc has been established, direct heated is not required. The filament has often burned out in the middle of an experiment without causing any interruption. Indirect heating by the arc is sufficient to maintain electron emission from the filament.

The magnet coil is cooled directly by a closed loop freon ~~F~~ 113 cooling system. The aperture and the plasma cup are attached to the magnet housing and are cooled by conduction. Deionized cooled water flows through the hollow structure of the intermediate electrode.

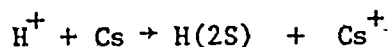
The beam is extracted through a 21 mil by 50 mil canal into a 70° plasma cone. This geometry is the result of years of empirical testing by J.L. McKibben and his associates at the Los Alamos Scientific Laboratory. It would seem that this source should produce more intense final beams, but the effect of space charge ~~is~~ to cause the

beam to expand radially. The presence of caesium vapour leads to partial space charge cancellation. Beam diagnostics in this area are difficult to perform. It would be possible to study the characteristics of the positive duoplasmatron beam, but this beam has much different properties if there is caesium vapour present. In the presence of caesium, positive and negative ions will be produced plus ground state and metastable neutral atoms. This multiplicity of beam particle species makes it difficult to identify and study any one part of the beam.

There are two approaches to alignment of this type of system. The usual concept is to provide fixed mechanical means of alignment or to use optical methods. At McKibben's suggestion, and following his design of the Los Alamos source, we have made provision to vary the position of the accel and decel electrodes in the X,Y, and Z directions while the source is operating. This usually increases the final beam intensity over that achieved with preset optical alignment. It is not possible to steer or focus the neutral beam coming out of the caesium canal. These mechanical adjustments of the electrode position provide the only way to steer the beam until after charge exchange takes place in the argon canal.

The Caesium Cell:

Generation of metastable H(2S) by the reaction



was first described by B.L. Donnally et al.⁽⁹⁾ in 1964. This paper plus his subsequent paper on the argon charge exchange process⁽¹⁰⁾ provided the basis for the first practical Lamb Shift ion sources.

In 1974, Pradel et al.⁽¹¹⁾ published an elegant study of this process. Their measurements indicate a maximum efficiency for H(2S) production at an energy of 0.5keV for the incident ions. At this energy, 30% of the total outgoing beam is in the form of H(2S) atoms for a caesium target thickness of about 10^{14} atoms/cm². It is interesting to note that Pradel's data indicate a rather sharp peak in the cross section. The original data presented by Donnally in 1964 indicated a relatively constant value for the cross section in this energy range. The process is expected to be velocity dependent and therefore an energy of about 1 keV should produce the maximum metastable fraction for a deuterium beam. This is confirmed in the operation of the source. However, the Los Alamos laboratory has found a best value for triton operation at about 600 eV rather than the expected 1.5 keV.

The thickness of the caesium target is controlled by separate heaters on the reservoir and the canal. It is believed that a crust of caesium compounds can form on top of the caesium between runs. This layer can be broken by heating. It is often necessary to heat the reservoir to almost 185°C. before setting optimum temperature levels at between 95°C. and 105°C. in both the reservoir and the canal. At these temperatures, the vapour pressure of caesium is about 5×10^{-4} torr. Proper operating conditions may be checked by observing the appearance of the beam as seen through a 1/4" hole in the side of the canal. A blue-pink glow is produced when the beam passes through the caesium vapour.

The Ion Deflection System:

The original design provided a set of electrostatic deflectors just after the caesium canal to steer the unwanted charged particles off axis. Insulated segments of the spin filter cavity can also be used to provide an electrostatic deflection field perpendicular to the beam axis. The direction of this deflection can be rotated. The field strength must not be too high, as quenching of the metastable beam will result. Best operation has been achieved with zero voltage on the deflector plates and about 200 volts across the spin filter segments. A second system has been incorporated into the source to control the charged ion beam. A copper tube $3/8$ " in diameter and $1\ 1/4$ " long has been mounted between the caesium cell and the first deflection plates. A negative potential of up to 10 volts is applied to the tube. A negative potential of 60 volts is applied to all four segments of the first deflector plates. This graded retarding potential tends to remove the low energy electrons from the particle beam. It is believed that space charge effects cause the negative ion beam to defocus so that it is dumped on the first aperture past the argon cell. The neutral beam of metastable atoms drift through this region unaffected.

The Spin Filter:

The "spin filter" is a complex device first described in 1968 by McKibben, Laurence and Ohlsen⁽¹²⁾. Its operation is based on the work of Lamb and Retherford published in 1951-52⁽¹³⁾. The filter is a copper radio frequency cavity 25 cm long. It is split into four longitudinal segments. (See figure 6).

R.F. power ($\approx 1\text{mW}$) at about 1.6 GHz is fed into the cavity, which resonates in a TM_{010} mode (i.e. longitudinal electric field). A potential of about 200 volts D.C. is applied across a pair of the cavity segments to provide a small D.C. field transverse to the beam axis. All of this is surrounded by a long solenoidal coil which provides a homogeneous axial magnetic field of about 5.75×10^{-2} Tesla.

In order to discuss the theory of this device, one must first review the structure of energy levels in the hydrogen and deuterium atoms. The area of interest involves the energies of the $2P_{1/2}$ and the $2S_{1/2}$ levels and their variation with magnetic field in the range, zero to about 6.0×10^{-2} Tesla. This information is presented in the Breit-Rabi diagrams for hydrogen and deuterium (figures 4 & 5). The values of m_I and m_J for each level in the high field limit, are indicated along the right hand side of the figures. The notation of the states as α , β , e , and f follows the convention used by Lamb and Retherford. There are a number of important features to note. The first is the depression of the energy of the $2P_{1/2}$ levels. This results in the crossing of the β and e levels at about 5.75×10^{-2} Tesla. The dipole selection rules (given below) allow the $2P_{1/2}$ atoms to rapidly decay to the $1S$ ground state levels. The lifetime is sufficiently brief that the e levels have a width of about 100 MHz. The $2S_{1/2}$ levels cannot decay to the ground state by single photon emission.

The $2P_{1/2}$ and $2S_{1/2}$ energy levels should be degenerate according to Dirac's theory of the hydrogen atom. The energy difference of 1.058 GHz, measured experimentally by Lamb and Retherford in 1950⁽¹³⁾,

HYDROGEN BREIT-RABI DIAGRAM

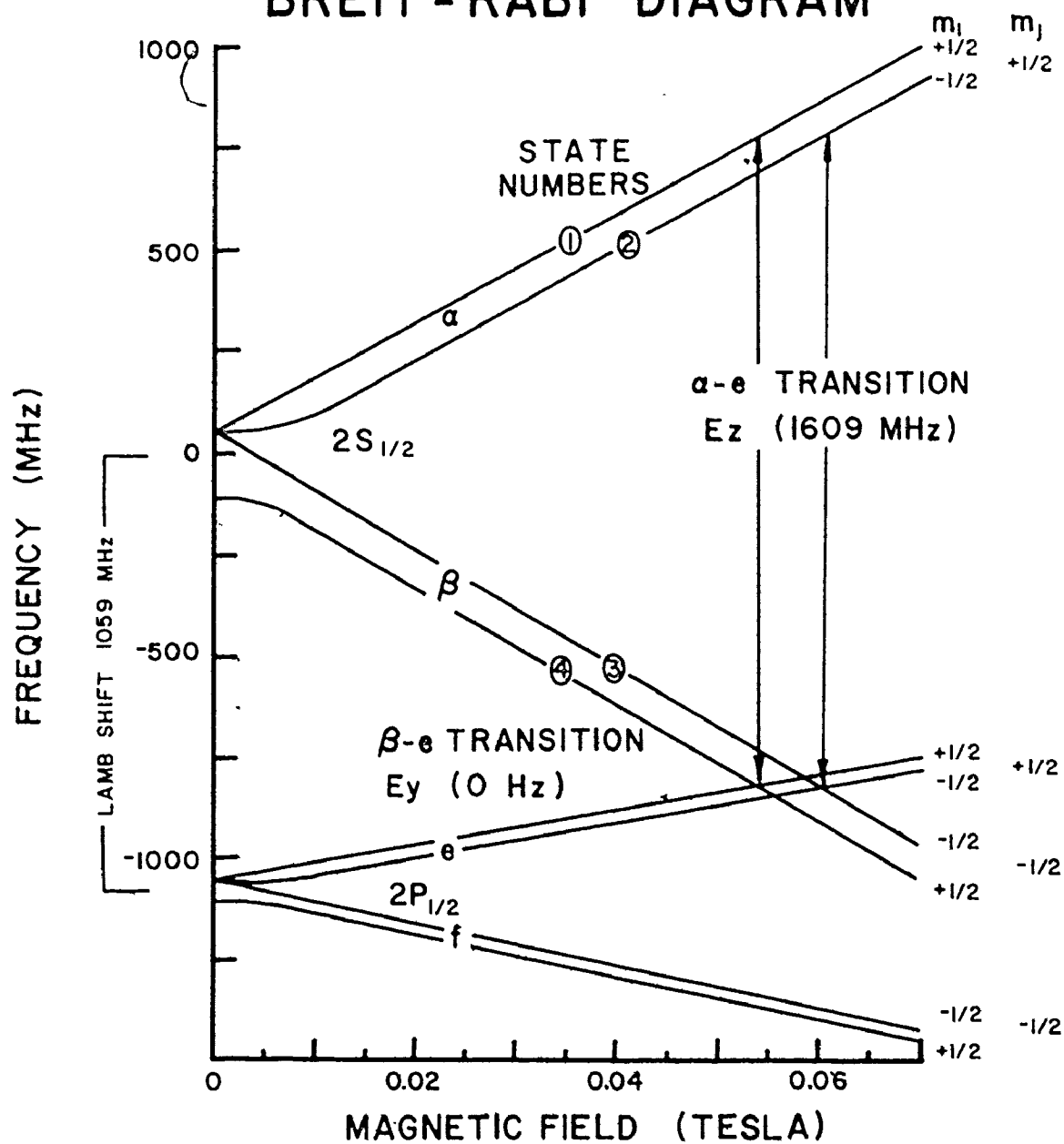


figure 4

DEUTERIUM BREIT-RABI DIAGRAM

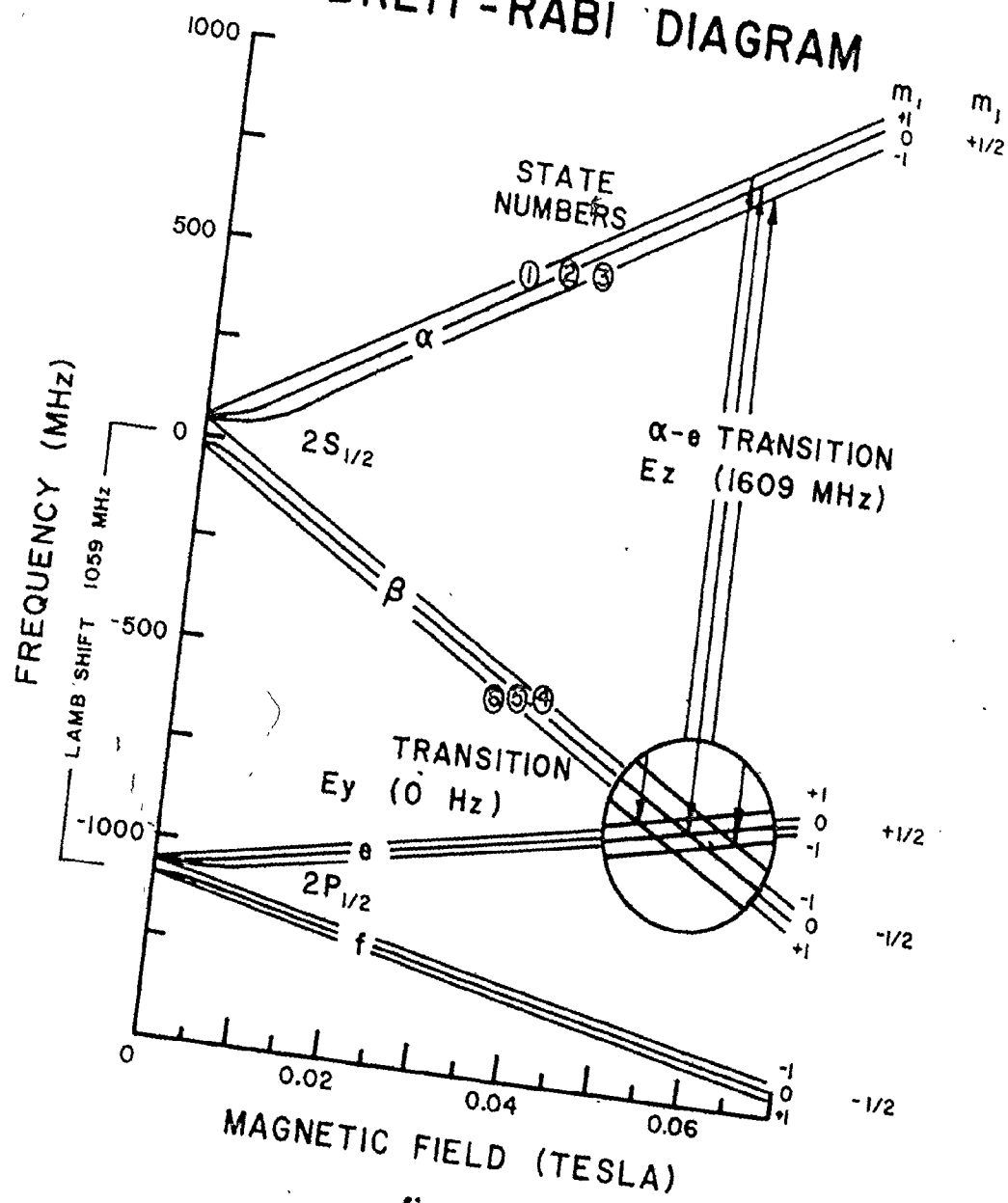


figure 5

was explained on a theoretical basis by Bethe⁽¹⁴⁾ using quantum electrodynamics. An interesting qualitative description of the Lamb Shift was originally proposed by T.A. Welton,⁽²¹⁾ and was mentioned in discussions at this laboratory*. The electron is smeared out due to recoiling from its virtual photon field and therefore resides in a sphere in space. The positions of the centers of these spheres would give the same calculated energy, but averaged over the vibration sphere, a greater time is spent outside the nominal orbit by the S state electron due to simple geometric effects (i.e. the curvature of the S orbit cuts a smaller portion out of the vibration sphere). This generates the higher average energy of the S state electrons that is known as the Lamb Shift. (See figure 7.)

The Hyperfine structure of the $2S_{1/2}$ and $2P_{1/2}$ states can be described by the Breit-Rabi formula.

$$W = \frac{-\Delta W}{2(2I+1)} + \frac{\Delta W}{2} \left(1 + \frac{2m_f}{I+1/2} X + X^2 \right)^{1/2} + \epsilon \Delta W X m_f \begin{matrix} + \text{ for } F=I+1/2 \\ - \text{ for } F=I-1/2 \end{matrix}$$

where $X = B/B_1$

$$B_1 = \Delta W(1+\epsilon)/g_J \mu_0$$

$$\epsilon = 1/\left(\frac{1836.1 g_J}{g_I} - 1\right)$$

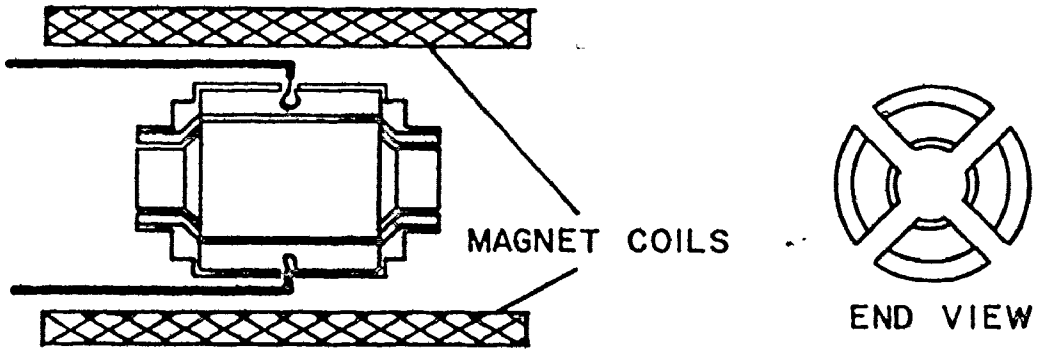
g_J = Lande g factor

μ_0 = Bohr magneton

B = magnetic field

ΔW = zero field hyperfine splitting

* The author is indebted to R. Summers-Gill, J. Panar and O. Straume for pointing out this argument.



- ↔ R.F. ELECTRIC FIELD
- ← D.C. MAGNETIC FIELD
- ↑ D.C. ELECTRIC FIELD

SPIN FILTER CAVITY

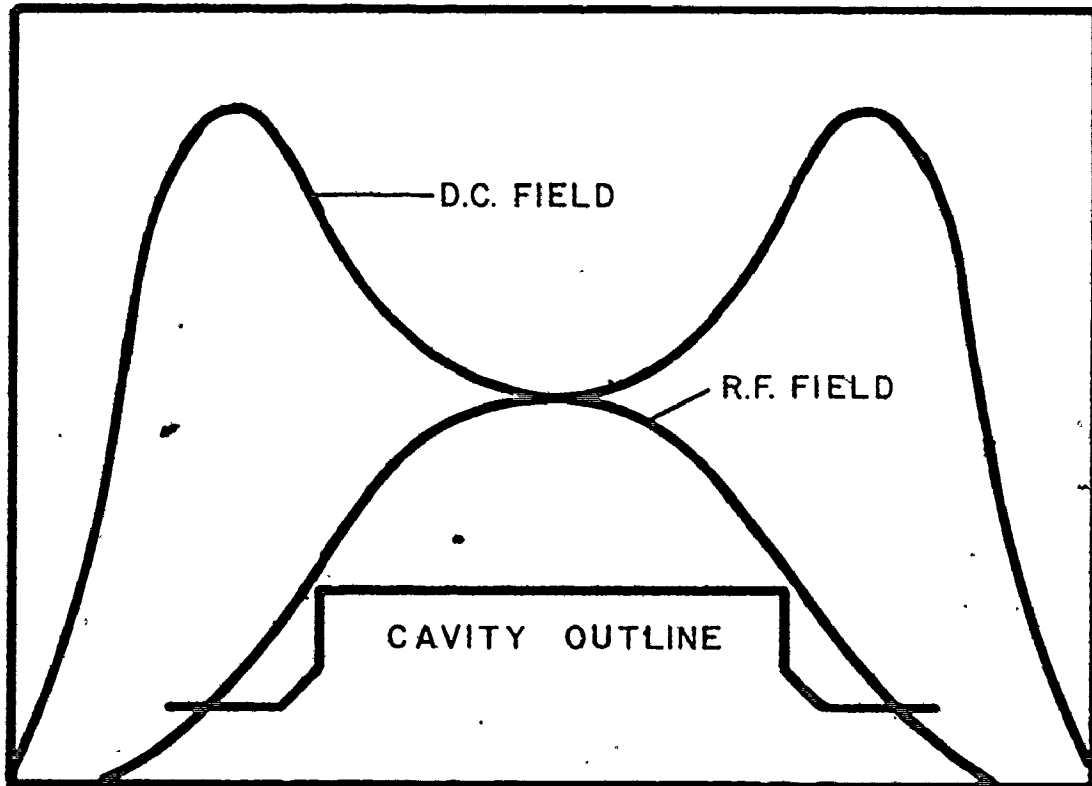


FIGURE 6 SPIN FILTER FIELDS

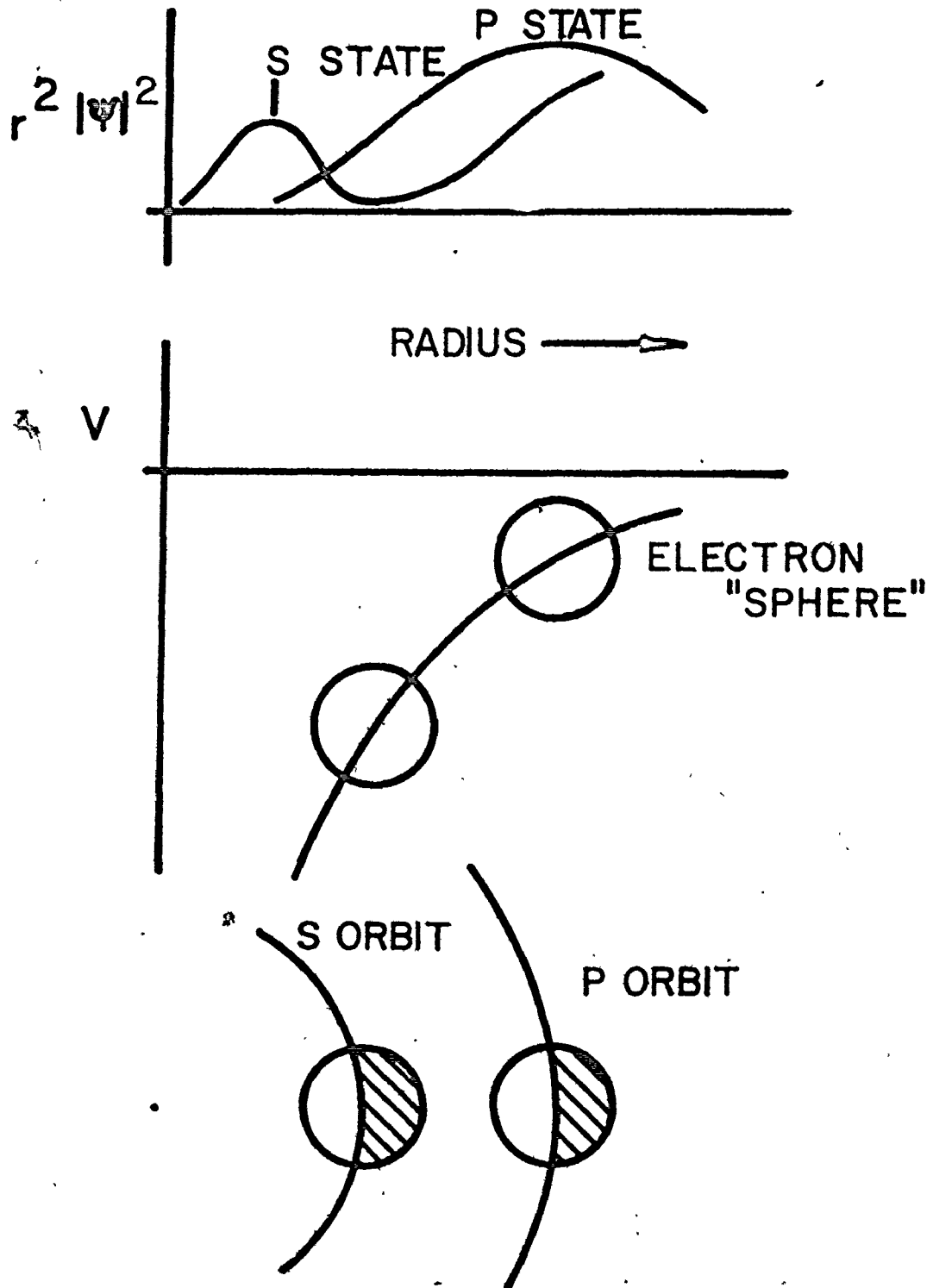


FIGURE 7 THE LAMB SHIFT

$$g_I = \mu_I / I = \text{nuclear } g \text{ factor}$$

$$m_f = m_J + m_I$$

Two Level Interactions - Selection Rules:

At this point, we can consider a number of possible two level interactions that describe the off resonance behaviour of the system. The electric and magnetic dipole selection rules in the region of interest are listed here. Since the magnetic field is in the region 5.75×10^{-2} Tesla, and is large compared to B_1 , it is most convenient to use an I, J, m_I, m_J basis rather than the I, J, F, m_F of the Breit-Rabi formula.

ELECTRIC DIPOLE OPERATOR ($-\vec{e}\vec{r}$)

\therefore odd, Δl must be odd. It can be shown that

$$\Delta l = \pm 1 \text{ since } \vec{r} \text{ is a linear combination of } Y_{1,m}$$

$$\Delta J = 0, \pm 1; \Delta m_J = 0, \pm 1; \Delta m_I = 0$$

If $\Delta m_J = 0$, the electric field required to induce transitions is parallel to the quantization axis, and if $\Delta m_J = \pm 1$ electric field must be perpendicular to the quantization axis.

MAGNETIC DIPOLE OPERATOR ($\vec{\mu}$)

$$\therefore \Delta l = 0$$

$$\Delta J = 0, \pm 1; \Delta m_J = 0, \pm 1; \Delta m_I = 0$$

$$\text{or } \Delta m_I = 0, \pm 1 \text{ and } \Delta J = \Delta m_J = 0$$

This latter combination can be ignored as it requires applied power levels that are much too high to be of importance in this context. If $\Delta m=0$, the magnetic field is parallel to the quantization axis, and if $\Delta m=\pm 1$, the required field is perpendicular to the quantization axis.

The $\alpha \leftrightarrow e$ transitions can be induced by a 1.6 GHz R.F. electric field parallel to the quantization axis (i.e. the magnetic axis). The β & e state energies are degenerate at $5.75 \times 10^{-2} T$ and can be coupled by a field of a few volts per centimeter perpendicular to the quantization axis. The e states have a half life of 1.6 nsec and therefore have a width of 100 MHz. Thus all α & β states can be coupled to the e states and hence decay rapidly to the ground state. Due to the width of the e states, this is a good approximation to the transition systematics off resonance.

The Three Level Interaction:

To understand the on-resonance selection (or survival) of a given m_I substate, it is necessary to consider at least three levels interacting simultaneously. (This is not a totally accurate treatment, but the effect of further levels is in the character of a perturbation.)

A complete, rigorous treatment of this problem has been published by Ohlsen and McKibben,⁽¹⁵⁾ however, it is worthwhile to discuss it in a more approximate way. The general equations describing the three level interaction may be written as follows: (after Ohlsen & McKibben)

$$i \dot{a} = \frac{1}{2} R_{\alpha e}^* e^{i(\delta + \omega_{\beta e})t} + \frac{1}{2} M_{\alpha e}^* e^{i\delta t}$$

$$i \dot{b} = V_{\alpha e} e^{i\omega_{\beta e}t} + \frac{1}{2} M_{\alpha e} e^{-i\delta t}$$

$$i \dot{c} = \frac{1}{2} R_{\alpha e} e^{-i(\delta + \omega_{\beta e})t} + V_{\alpha e} e^{-i\omega_{\beta e}t} - \frac{1}{2}(i\gamma c)$$

where

$$\delta = (\omega_{\alpha\beta} - \omega)$$

$\omega_{\alpha\beta}$ is the frequency separation of the α and the β states

ω is the frequency of the radio frequency field

$R_{\alpha e} = R e^{i\delta_0}$ (R is the matrix element for the electric dipole interaction between the α and β states)

$M_{\alpha e} = M e^{i\delta_0}$ (M is the matrix element for the magnetic dipole interaction between the α and β state)

$\delta_0 =$ phase at time $t = 0$

V is the matrix element for the electric dipole interaction between the β and e states.

a, b, and c represent the amplitudes of the α , β and e states, respectively

At resonance, $\omega_{\beta e} = 0$ and we select $\omega = \omega_{\alpha\beta}$ (or more correctly $\omega_{\alpha e}$), and

$\delta = 0$. $1/2(i\gamma c)$ is a damping term describing the decay of the e state.

This gives:

$$i \dot{a} = \frac{1}{2} R_o^* c e^{i(0)t} + 1/2 M_o^* b e^{i(0)t}$$

$$i \dot{b} = V^* c e^{i(0)t} + 1/2 M_o a e^{i(0)t}$$

$$i \dot{c} = \frac{1}{2} R_o a e^{i(0)t} + V b e^{-i(0)t} - 1/2(i\gamma c)$$

The terms involving M_o and M_o^* may be neglected as magnetic interaction is much weaker than the electric interaction

$$i \dot{a} = 1/2 R^* c$$

$$i \dot{b} = V^* c$$

$$i \dot{c} = 1/2 R a + V b - 1/2(i\gamma c)$$

Differentiating the third equation and substituting from the others

$$\ddot{c} + 1/2 \gamma \dot{c} + P^2 c = 0 \quad \{P^2 = 1/4 R^* R + V^* V\}$$

The general solution is $c = C_1 e^{-\mu_1 t} + C_2 e^{-\mu_2 t}$

where μ_1 and μ_2 are the two roots of

$$\mu^2 - 1/2 \gamma \mu + P^2 = 0$$

$$\mu_{1,2} = \gamma/4 \pm \sqrt{(\gamma/4)^2 - P^2}$$

To evaluate the constants we can assume the initial conditions;

$$(a = 1, b = c = 0) \text{ at time } t=0$$

$$\therefore \dot{c} = -1/2 i R \text{ at } t=0$$

we obtain then $a = 1 - \frac{R^* R}{4P^2} + \frac{R^* R}{8\eta} \left(\frac{e^{-\mu_2 t}}{\mu_2} - \frac{e^{-\mu_1 t}}{\mu_1} \right)$

$$b = -\frac{V^*R}{2P^2} + \frac{V^*R}{4\eta} \left(\frac{e^{-\mu_2 t}}{\mu_2} - \frac{e^{-\mu_1 t}}{\mu_1} \right)$$

$$c = \frac{iR}{4\eta} (e^{-\mu_1 t} - e^{-\mu_2 t})$$

$$\text{where } \eta = \sqrt{(\gamma/4)^2 - P^2}$$

∴ the real parts of μ_1 and μ_2 are positive for all P^2 , the exponential terms decay to zero after sufficient time, to finally give; (as an asymptotic solution)

$$a \rightarrow \frac{V^*V}{1/4 R^*R + V^*V}$$

$$b \rightarrow \frac{-1/2 V^*R}{1/4 R^*R + V^*V}$$

$$c \rightarrow 0$$

$$\text{and } 1/2 Ra + Vb = 0.$$

Lamb and Retherford⁽¹³⁾ summarized as follows; "An examination of the solution reveals that after damping of transients this relationship [1/2 Ra + Vb = 0] is satisfied, and the state oscillates between a and b with such phase and amplitude relations that the decaying state c is not excited".

The construction of the RF cavity is such that the RF field strength varies as $\sin(\pi z/z_0)$ where z is the distance along the beam path from the entrance of the RF region and z_0 is the total length. V , the DC field strength is largest at the ends of the

cavity. Since $|R|$ is slowly decreased to zero, the α and β mixture will be transformed into a pure α state.

Also, any β state particles existing prior to the spin filter will be quenched to the ground state by deflection fields before or at the beginning of the RF cavity.

Thus as the particles enter the argon charge exchange region, only α state metastable and ground state atoms will survive. The ratio $|R|/|V|$ determines the equilibrium population of the α and β states in the spin filter region, but as stated above, this ratio varies in such a manner that all metastables are in the α state as they leave the spin filter.

The metastable beam transmission through the spin filter system as a function of magnetic field is characterized by a broad region of quenching due to the two level interactions. In this region, the metastable atoms are quenched to the ground state. Two narrow peaks in the case of protons or three in the case of deuterons, occur at the magnetic field values corresponding to the three level resonant interaction. At these points, the quenching of an individual α state is suppressed and atoms of that state pass through the filter. The magnetic field values for transmission of individual states are as follows:

$$\text{H}(2\text{S}) \quad m_I = + 1/2 \quad \text{at } 0.0539 \text{ T}$$

$$m_I = - 1/2 \quad \text{at } 0.0605 \text{ T}$$

$$\text{D}(2\text{S}) \quad m_I = + 1 \quad \text{at } 0.0565 \text{ T}$$

$$m_I = 0 \quad \text{at } 0.0575 \text{ T}$$

$$m_I = - 1 \quad \text{at } 0.0585 \text{ T}$$

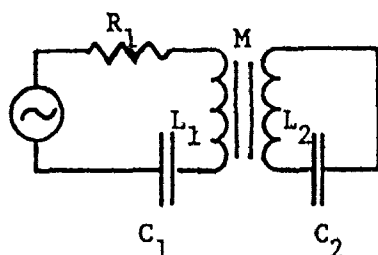
Various Views of the Three Level Interaction:

The three level interaction is difficult to picture in terms of simple concepts. Here are three analogies which may assist in understanding the phenomena.

1. The Optical Metaphor:

This is not a very precise analogy but as optical interference patterns are a commonly experienced thing, they may be called on as an example of two phenomena combining in a coherent fashion to produce an interference effect.

2. An Electrical Analogy;



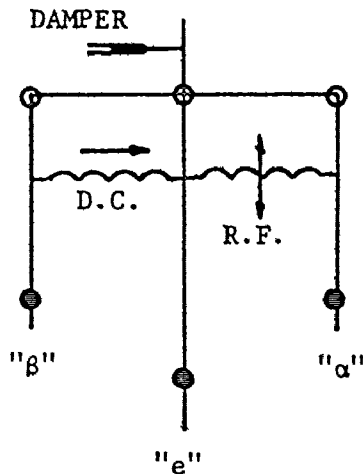
This analogy of a pair of coupled resonant circuits was suggested by Lamb and Retherford. The primary circuit has parameters L_1 , C_1 , and R_1 . The lossless secondary (L_2 and C_2) is coupled to the first by a

mutual inductance M . The α transition is represented by $\omega_1(L_1 C_1)^{-1/2}$ and R_1 represents radiation damping. The second circuit resonates at a frequency $\omega_2 = (L_2 C_2)^{-1/2}$. This is the equivalent of the transition frequency $\omega_{\alpha\beta}$, between the α & β states. The β state does not decay directly and this is represented by the zero resistance of circuit two. There is no direct coupling between states α & β (except by relatively weak magnetic dipole radiation). In the electrical analogy, the second resonator is excited only by its mutual inductive coupling to the first circuit. In the atomic case, the DC electric

field couples the β & e states. The power absorption of this circuit has a broad resonance for $\omega \sim \omega_{\alpha e}$ while in a narrow band about $\omega = \omega_{\alpha\beta}$, the reflected impedance of the lossless secondary is large and reduces the response of the network.

3. The Triple Pendulum:

An elegant mechanical analog to the three level interaction has been constructed by J.L. McKibben.⁽¹⁶⁾ It consists of three pendula connected by springs as shown in the drawing. The central pendulum (representing the "e" state) has a damping mechanism to represent decay to the ground state. A spring connects the " β " pendulum to the "e"



representing the transverse D.C. field.

Similarly the " α " pendulum is connected to the "e" by a spring representing the R.F. field. The resonant condition can be represented by adjusting the lengths of the pendula so that the " α " and " β " swing out of phase transferring no energy to the "e" pendulum. If one pendulum is put just off resonance, decay will occur through the "e" state. The position of the R.F. spring can be changed to represent variation of the coupling with time. The vibration amplitude will be all transferred to the " α " pendulum as the RF is "turned off". This is similar to the change in state populations as the metastables leave the spin filter.

In the Spin Filter, the differential equations are first order instead of second as in the case of the pendula, but in both cases the

square of the amplitude is involved in the energy.

All of these analogies are inexact as they try to explain the phenomena by reference to simpler situations. However, I believe that they are useful aids to help in understanding the interaction as long as we remain aware of their limitations.

The Four Level Problem:

Referring to the Breit-Rabi diagram, it will be noted that the f levels are reasonably close to the levels of interest. These levels are weakly connected in that an α - f transition will be induced by the transverse electric field, and the β - f transition by the longitudinal R.F. field.

These interactions are important as a quenching mechanism (see next section). In all, the fourth level will not cause the equilibrium ratios of the α & β to change, but the amplitude will decrease. This implies that the field strengths should not be too high and the length of the spin filter should be as short as possible.

Quenching:

Quenching is simply the effect of any interaction that will cause the metastable beam to decay to the ground state. It can be caused in many ways, inadvertently, or intentionally to measure the size of the metastable beam. There are three major quench mechanisms available in the spin filter region. Increasing the D.C. or the R.F. fields to high intensity will quench the beam through the f levels. A so-called B quench occurs when the magnetic field is moved just off the resonance peak. The polarization is (in first

order) related to the quench ratio by the following formula:

$$P = 1 - 1/Q \quad (Q=I(\text{total})/I(\text{quenched}))$$

Errors of up to 5% are possible, because the quench ratio is a measure of the metastable portion of the beam, not directly the polarization. The polarization may differ for a number of reasons. The field in the argon cell alters the state populations as discussed later. The direction of the polarization axis also depends on a correct setting of the precessor. Finally, the background beam is in fact slightly polarized in the opposite sense to the chosen beam.

Diagnostic information can be obtained by comparing the different quench ratios. The usual quench measurement at our laboratory, is the delta B quench. If the RF level is too low, the quench ratio between peaks will be lower than that obtained above or below the peaks. Comparison of the delta B quench with the E quench (effected by raising the Spin Filter transverse DC field voltage to 1000 volts) enables one to infer the contribution to total beam current from negative ions generated in the caesium canal. If source steering and focusing is incorrectly set, such negatives can be accelerated. In fact, beams of unpolarized ions, an order of magnitude larger than the polarized beam can be observed. The E quench not only causes decay of the metastable beam, but also deflects all ions produced before the spin filter. Therefore it is important to tune the source so that the delta B and the E quenches are identical. This insures that no direct negative beam is being accelerated.

The RF quench method has not been used in our lab because of difficulties with the technique in the case of $m_I=0$ deuterons, a beam of particular interest to us. The electron cyclotron frequency at the magnetic field required to choose $m_I=0$ is very close to the RF frequency. Electron cyclotron resonance can be initiated by electrons released by the beam striking molecules of residual gas in the spin filter region. Absorption of up to 98% of the applied RF power is possible. This puts a very heavy load on the RF power circuitry. It is difficult to achieve steady conditions, and also to provide sufficient RF power. This problem also requires that the RF power be kept fairly low when selecting this state. Once electron resonance begins, it builds up catastrophically and the polarization is destroyed.

The location of the Faraday cup used to make the quench measurements is important. The polarized beam is generated on axis. The background beam results from multiple collisions and from off axis components. This means that the emittance of the polarized component is superior to that of the background beam. Therefore, every time the beam goes through a slit or aperture, more of the background beam, than the polarized beam is removed, and the polarization actually improves. It is important to measure the polarization at the target position for use in data analysis, but measurement closer to the source is better if you are trying to check for problems in the source as opposed to problems related to the accelerator.

Definitions of Quenching Parameters:

Quench Ratio; $Q = \frac{I_p + I_b}{I_b}$

where I_p is the intensity of the polarized current
and I_b is the intensity of the background (or
quenched) current.

for protons: $P_3 = \frac{N_+ - N_-}{N_+ + N_-}$

where N_+ is the number of particles in the $m_I = +1/2$
states and N_- is the number of particles in the
 $m_I = -1/2$ state.

$$P_3 = \frac{Q - 1 + 1/2 - 1/2}{Q}$$

$$= \frac{Q - 1}{Q} = 1 - \frac{1}{Q}$$

for deuterons: $P_3 = \frac{N_+ - N_-}{N_+ + N_- + N_0}$

where N_+ is the number of particles in the $m_I = +1$ state
 N_- is the number of particles in the $m_I = -1$ state and
 N_0 is the number of particles in the $m_I = 0$ state.

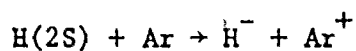
$$P_3 = \frac{Q - 1 + 1/3 - 1/3}{Q}$$

$$= 1 - \frac{1}{Q}$$

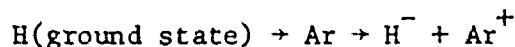
$$\begin{aligned}
 P_{33} &= \frac{-2N_0 + N_+ + N_-}{N_0 + N_+ + N_-} \\
 &= \frac{-2(Q - 1 + 1/3) + 1/3 + 1/3}{Q} \\
 &= \frac{-2Q + 2 - 2/3 + 2/3}{Q} \\
 &= -2 \left(1 - \frac{1}{Q}\right)
 \end{aligned}$$

The Argon Cell:

In 1965, Bailey Donnally published evidence to show that a thin argon target would produce the reaction, ⁽¹⁰⁾



at a higher rate than the reaction,

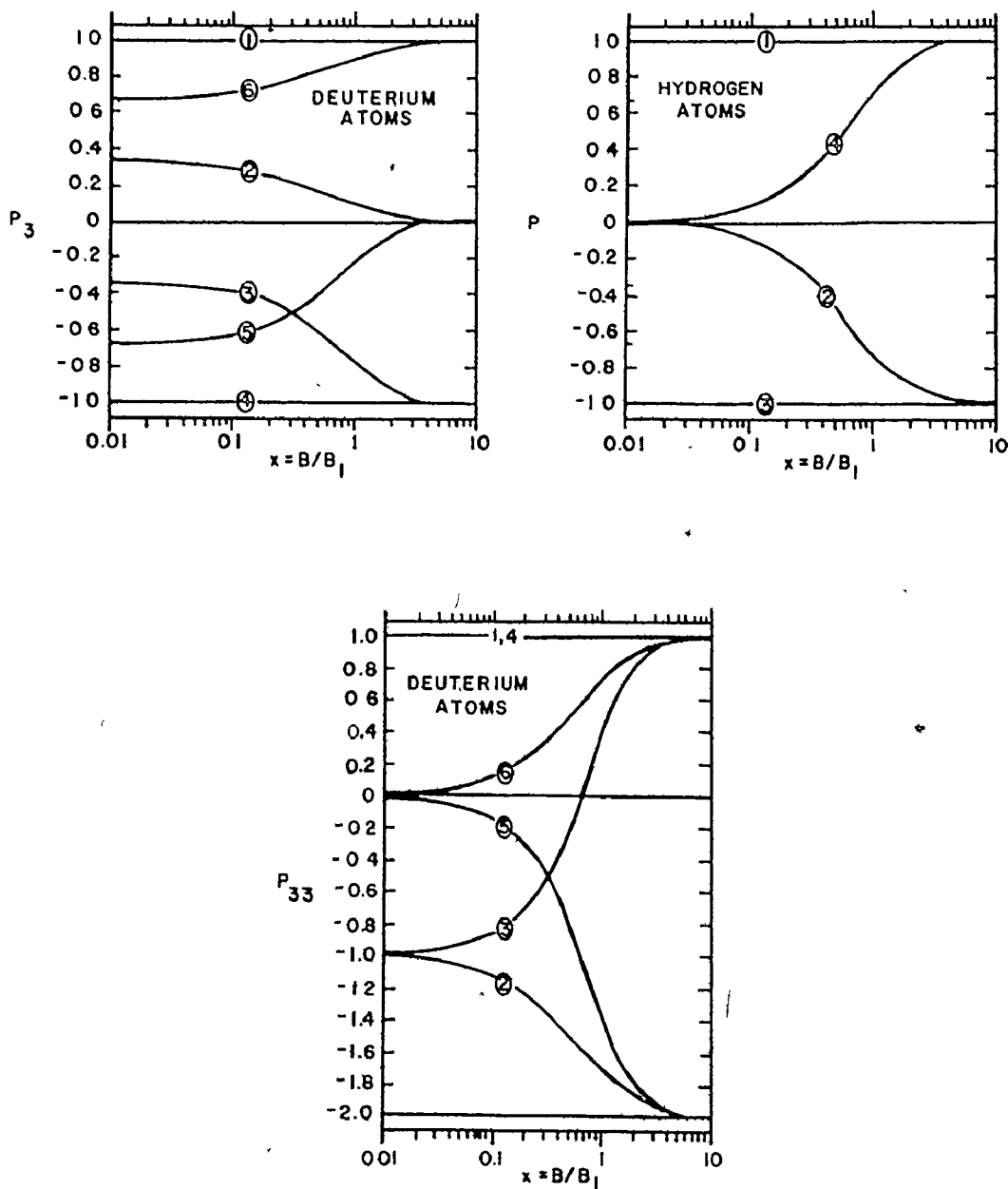


for atoms in the range of 500 eV (or 1000 eV for deuterons).

This discovery led to the successful design of the Lamb Shift type polarized ion sources. The output of the Spin Filter is a large number of more or less unpolarized ground state atoms plus a small component of polarized H(2S) atoms. The argon adding process is sufficiently selective (i.e. by a ratio of 100:1) that we can preferentially pick out the polarized component of the atom beam to form negatives for injection into the tandem accelerator. Donnally's data suggest that this process is sharply peaked at a velocity equivalent to a proton energy of 500 eV. It would appear that his measurements were in fact sensitive to both the H(2S) production cross-section in caesium vapour and the argon electron adding cross-

section simultaneously. The more recent work of Pradel mentioned earlier, would suggest that the sharp peak is an artifact of the H(2S) yield rate. A large flow of argon (of the order of one standard cubic centimeter per minute) is required due to the large diameter of the beam and the canal. It has been difficult in the past to provide adequate pumping speed to dispose of this gas load. At the suggestion of Dr. McKibben, two helium cryopumps were installed at the ends of the argon canal as pumps. This scheme has also been incorporated in the new triton polarized source at L.A.S.L. The details of the cryopump system were described by this author in an earlier presentation⁽¹⁷⁾. "Cryodyne model 20" helium refrigeration units supplied by Cryogenic Technology Incorporated are used to cool the pumping surfaces to about 20° Kelvin. An intermediate stage at 70 to 80° Kelvin, covered with aluminized mylar is attached to the first stage of the cold head. This heat shield is required to reduce the heat load on the 20° Kelvin stage.

The change in vector and tensor polarization at low magnetic field is shown in figure 8. While all possible α & β states are shown in these diagrams one should recall that only the α are transmitted by the spin filter. That is states 1 & 2 for hydrogen, and states 1, 2 & 3 for deuterium. For best polarization, ionization should take place at high fields, but serious beam emittance degradation would occur as the now charged particles leave the magnetic field. In practice, a field of about 6×10^{-4} T is used for state one deuterons and protons. Approximately 6×10^{-3} is required for state 2 ($m_I = 0$) deuterons to maintain maximum tensor polarization.



SPIN STATE POLARIZATION

figure 8

Pure vector polarized deuterons can be obtained from state three atoms by carefully choosing the argon field to be about $B/B_1 = +0.7$. At that value of magnetic field, the tensor polarization is zero and the vector polarization has a theoretical value of $P_3 = -0.7$.

The parameter $x = B/B_1$ is defined as follows:

B = magnetic field

$$B_1 = B_0 / (1-k)$$

$$= 6.34 \times 10^{-4} \text{ T for H(2S)}$$

$$= 1.46 \times 10^{-4} \text{ T for D(2S)}$$

$$k = g_I / (1836 g_J) = 1.520 \times 10^{-3} \text{ for H(2S)}$$

$$= 0.233 \times 10^{-3} \text{ for D(2S)}$$

CHAPTER III
OPERATIONAL PROCEDURES

Introduction:

Unlike the operation of usual sources, this device's performance cannot be monitored simply. Performance of the tandem systems in general, is adjusted to attain maximum beam current at the Faraday Cup or target. However, the quality of a polarized beam is dependent on two parameters, the current, and the polarization.

A suitable figure of merit for both proton and deuteron beams was discussed in a paper by Keaton and Ohlsen ⁽¹⁸⁾ of Los Alamos. The most useful beams are achieved by maximizing $p^2 I$ where p is the beam polarization and I is the beam intensity. It is usual that maximizing either polarization or current, will cause a decrease in the other. In addition, the polarization is not easily measured. The usual, related parameter, that can be quickly measured, is the "quench ratio". This is defined as the on resonance current divided by the off resonance current. The relationship of this parameter to the polarization is discussed elsewhere. These difficulties result in a device that cannot be operated without some considerable understanding of its theory of operation and therefore, of the ways in which the control functions interact. It is the purpose of this section to give some guidelines to the operating researcher who has had some training and experience with the source.

The Duoplasmatron System:

Experience to date has shown that this system is relatively trouble free once it has reached normal operating conditions. The arc in the source is an order of magnitude more intense than that in our regular source. Thus instabilities can have a much more catastrophic effect due to the power levels involved.

Before the run starts, it is usual to clean the intermediate electrode, the aperture and the plasma cup. The filament should be replaced or, at least, recoated. This "clean" assembly must be outgassed for at least a couple of hours before an arc is initiated. Failure to do so will cause severe erosion and filament failure from heavy contaminant ions in the arc. The filament current should be increased in stages from about 20 amps to about 40 amps. The sourcehead pressure with the bypass open should not be allowed to exceed 500 microns. The current should not be increased until the pressure drops below 100 microns at each stage of outgassing. Next, a flow of source gas can be introduced and an arc initiated (by a brief increase in filament current). The arc current should be held to less than four amps by reducing the arc voltage until the pressure stabilizes. The gas valve must be adjusted to maintain a pressure of about 100 to 200 microns in order to sustain the arc. At this point the bypass can be closed, and the source set to its regular operating parameters. It will be noticed that the gas pressure is very sensitive to all other adjustments. This is due to the pumping action of the plasma which can draw large amounts of gas through the aperture. The magnet setting is especially critical

in this respect. In fact it should be set to about 7.8 to 8.0 amps and left there. If the filament burns out, after the arc has been struck, the arc will maintain itself as long as it is kept at a reasonable intensity. Excessive probe current is a symptom of arcing from the filament leads to the feedthrough flange. Extensive damage will result in short order if this condition is sustained.

The Accel-Decel System:

This is the system that extracts the beam and focusses it through the caesium canal. The geometry of the electrodes (including the plasma cup of the duoplasmatron source) was adopted by the Los Alamos group after much experimentation. The value of the accelerating voltage is determined by requirements of the metastable H₂S cross section in the caesium vapour. The usual settings of the neutral beam power supply are 550 volts for protons, and 1100 for deuterons. The setting of the extraction voltage is interdependent with the duoplasmatron magnet setting and the setting of the 30 KV power supply for the first pre-accelerating gap after the Argon cell. It will also vary depending on the longitudinal position of the electrode.

There are six accessible mechanical adjustments on the two electrodes. They can be moved in the X, Y, and Z directions. These are critical adjustments as it is the last chance to change the particle trajectories until after the argon adder canal. The electrodes are preset optically before the run. They are then optimized in an iterative process at each stage of beam transport. Due to the presence of caesium vapour in this area, you can actually see the beam profile

by looking through the windows closely.

The Caesium Canal:

It is this item that seems to be the cause of most operating troubles. The function is simple; to provide a low pressure caesium vapour target for the hydrogen or deuterium beam. If the target is too thin, the beam current will be low. If the target is too thick, multiple collision processes will adversely affect the ratio of metastable neutrals to ground state neutrals. The present design has two faults. The first is a long time lag to reach thermal equilibrium due to its mass (this does have the advantage that it prevents fast temperature drifts once the correct value has been achieved). The second fault is the operation of the reservoir valve. Remote mechanisms for closing and opening have not been reliable. In addition, it would appear that partial blockage of the caesium pathway sometimes occurs, or else the surface of the liquid caesium becomes coated with some substance that inhibits the escape of the vapour.

There are separate heaters and thermocouples for the canal and the reservoir. The best operation has been achieved when these are in the temperature range of 95°C to 110°C. There should be a noticeable pink-blue glow visible through the small port in the side of the canal.

When first starting up, it is often necessary to run the reservoir temperature up as high as 180°C to "wet in" the unit. A bright glow will appear quite rapidly in the canal when this happens. At this point the heater currents must be lowered to normal values. Beam polarization will improve as the usual temperatures are reached. If the caesium

glow disappears, this process may have to be repeated. If the source has to be opened for any reason, the caesium must first be allowed to cool. The slide valve must be shut to keep vacuum in the spin filter section, and then the source section may be let up to atmospheric pressure with dry argon gas. As soon as the unit has been opened, the caesium valve must be shut by hand. It should be reopened only just prior to pumpdown.

The Deflection Systems:

There are two modes of deflection used in this system. A voltage of about 200 volts on the D2 (spin filter) plates will impart sufficient radial velocity to the charged beam that it will be intercepted at the acceleration gap aperture (.120"). It is not possible to achieve 100% interception of the beam as this would require a higher voltage which would in turn quench some of the metastable beam. The direction of the deflection can be varied to advantage. This fact may be due to the spiral trajectory of the charged particles through the spin filter and argon cell regions.

A second mode of beam deflection makes use of space charge. A 3/8 inch tube at the exit of the caesium canal can be set at a potential of 0 to 15 volts negative. Similarly, the four D1 deflector plates can be offset up to about 100 volts. This retards the low energy electrons in the beam which then diverges rapidly. The remaining ion beam has an energy of 500 eV (for protons) and will not be retarded much. It will have a net positive charge and therefore similarly will blow up.

The Spin Filter System:

The operation of the Spin Filter system requires the setting of three separate fields. The "D2" deflection voltage described above also connects the β & e states. The Spin Filter is located in a solenoidal magnetic field. This field is generated by a large coil located outside the vacuum wall. It consists of a main coil and two trim coils. They are all canned in a stainless steel container and are directly cooled by a freon coolant. The current is provided by a programmable Kepco power supply. Field regulation of 0.05% is required in order to separate the substates. A pushbutton labelled "quench" provides a 3.5×10^{-3} T field change for rapid measurement of the metastable portion of the beam. The third field is the 1.6 GHz R.F. field with power of up to 10 watts provided by a "TRAK" oscillator. Varactor tuning allows some change in frequency to match the resonant frequency of the cavity. A power regulating system, based on a Hewlett Packard P.I.N. modulator, is controlled by a signal picked up by a small detector loop in the cavity. Operation is complicated by the presence of the cyclotron resonance near the $m_I=0$ substate selection condition. This was described in the section on quench ratio measurements. Good vacuum conditions and the use of R.F. intensities no larger than required for the three level interaction (i.e., about 0.2 mW measured in the cavity) can prevent the onset of this difficulty. Figure 9 is a block diagram of the system.

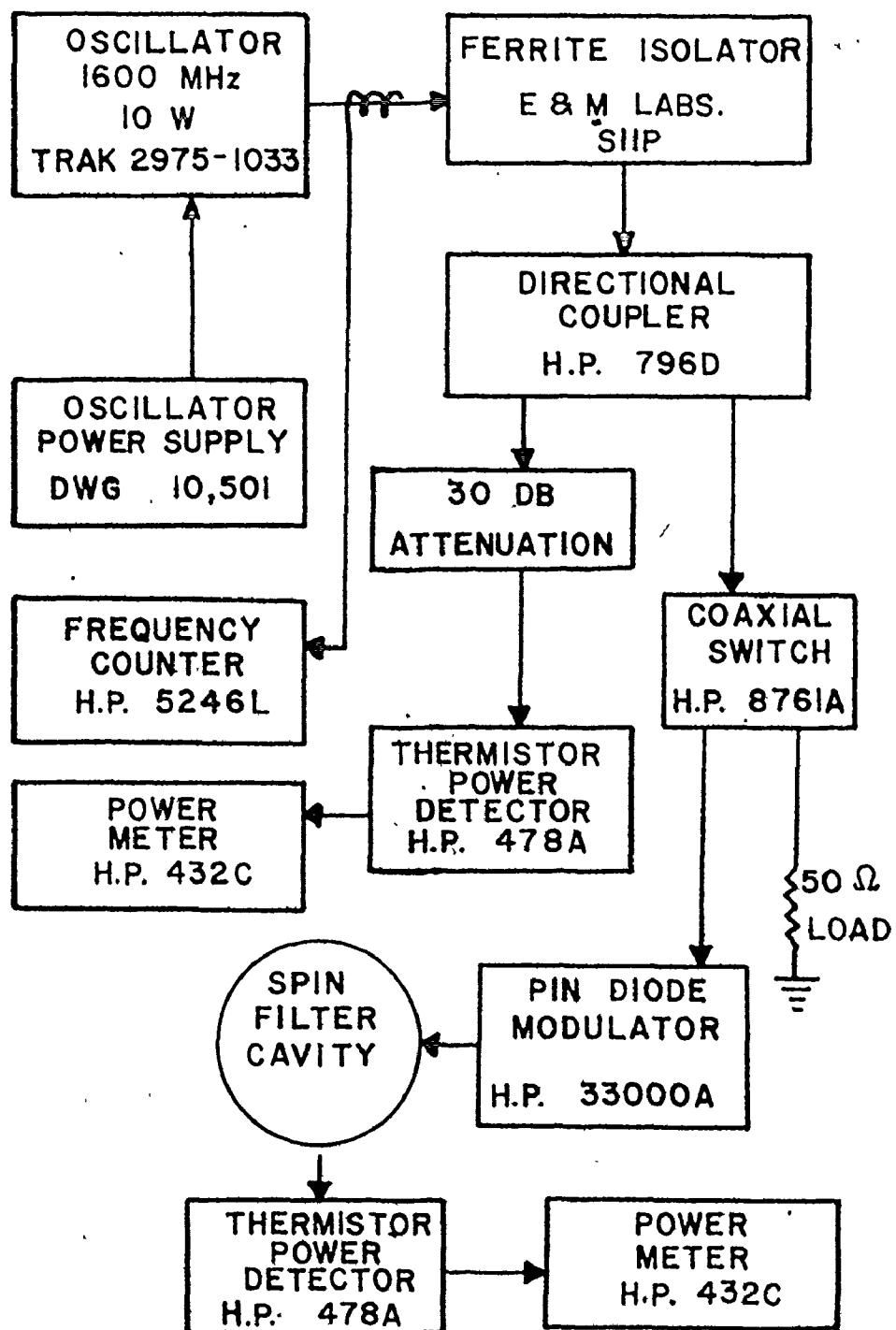


FIGURE 9
BLOCK DIAGRAM OF THE R.F. SYSTEM

The Argon System:

The major problem in the argon adder region, is the control of the large amounts of argon gas that must be pumped. Helium cryopumps were adopted for this task. The cryopumps must be started about four hours before argon flow is started. Once a temperature of about 20° to 25° Kelvin has been reached they are ready for use. A small current through grids in the cryopumps generates about 0.3 watts of heat in order to prevent buildup of solid argon near the beam.

The argon density is critical. Flow must be set carefully to maximize P^2I . The total current is not as sensitive to this thickness.

After some days of running, a layer of argon forms that is of sufficient thickness that the outermost layers are not cool enough. The vapour pressure from this layer will dominate the target thickness which will therefore no longer be controlled by the adjustment of the flow control. This also will result in charge exchange taking place outside of the desired region where the magnetic field is set to the proper values. At this point the cryopumps must be shut off and at least partially warmed up. This points out that the lowest the argon flow consistent with adequate beam is best. This will improve the P^2I , reduce scattering and prolong the period between cryopump warm-ups.

The Spin Precessor:

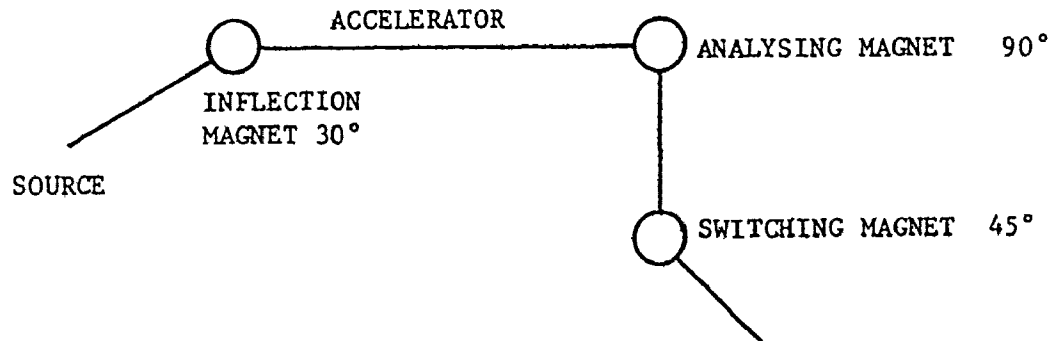
A device known as a "Wien Filter" is used to orient the spin axis in the desired direction. This axis will precess about the lines of magnetic field, thus the effect of the inflection, analyzing and switching magnets must be allowed for in determining the desired direction

for the spin axis as it leaves the precessor. In the case where the spin axis is required to be vertical at the target, these magnets will have no effect as their field lines will be parallel to the spin axis and no precession will occur.

If the polarized ion spends a given amount of time in a known magnetic field, the degree of precession can easily be calculated. In the precessor, it is required that the beam trajectory not be altered. Therefore an electric field perpendicular to the magnetic field is used to counter the $v \times B$ force of the magnetic field. The spin axis will precess as required. The "Wien Filter" can be rotated about the beam axis and thus, by selection of the appropriate combination of precessor fields and orientation, the spin axis may be directed in any way. The following is a sample calculation to show how the spin axis orientation is selected.

Determination of Spin Axis for $m_I = 0$ deuterons

Into ENGE with Z Axis in the Beam Direction



$$\text{Spin Rotation } \omega_s = g \frac{e}{2m_p} B$$

$$\text{Beam Deflection } \omega_k = \frac{e}{m_d} B$$

$$\text{+ve ion } \frac{\Delta\theta_s}{\Delta\theta_k} = \frac{g}{2} \frac{m_d}{m_p} - g = 0.857$$

-ve ion \rightarrow spin rotates opposite to beam deflection

Spin direction assuming no precession.

$$\text{after } 30^\circ (1 + 0.857) 30^\circ = 55.6^\circ \quad \text{left}$$

$$\text{after } 90^\circ (1 - 0.857) 90^\circ = 12.9^\circ \quad \text{left}$$

$$\text{after } 45^\circ (1 - 0.857) 45^\circ = 6.4^\circ \quad \text{right}$$

\therefore we must rotate 62.1° to the right in the precessor. (i.e. field polarity should be opposite to that of the inflection magnet).

Calculation of Spin Precessor Fields

Protons: Larmor frequency of spin precession

$$\omega_s = \frac{geB}{2m_p} \text{ rad/sec}$$

$$\text{for } 90^\circ \text{ precession, } \theta_{\text{rot}} = \pi/2 = \omega_s \times \ell/v$$

where ℓ = effective length of precessor
 = 47.3 cm.
 v = ion velocity

$$\text{therefore } \frac{\pi}{2} = \frac{geB}{2m_p} \ell/v$$

$$B = \frac{\pi}{2} \frac{2m_p}{ge\ell} C \sqrt{\frac{2E}{m_p C^2}}$$

$$B = 2.72 \times 10^{-3} \sqrt{E} \text{ Tesla}$$

E , the ion energy, in keV

$$V_{\text{tot}} = vBd$$

where (d = electrode spacing)

thus V_{tot} = total voltage on precessor = vBd

$$= \frac{2\pi Ed}{ge\lambda}$$

$$= 25 E \text{ volts}$$

Deuterons:

For deuterons $g = 0.857$ instead of 2.79 as for protons

$$\text{therefore } B = 1/2 \cdot 2.72 \times 10^{-3} \times \frac{5.58}{.857} \sqrt{E} \text{ Tesla}$$

$$= 8.85 \times 10^{-3} \sqrt{E} \text{ Tesla}$$

$$V_{\text{tot}} = \frac{5.58}{.857} \times \frac{25}{2} E$$

$$= 81.4 E \text{ volts}$$

for other than 90° multiply by $\frac{\theta}{90^\circ}$

Energy	Protons 90°		Deuterons 90°		Deuterons 62.1° *	
	B	V_{tot}	B	V_{tot}	B	V_{tot}
40 keV	1.72×10^{-2}	1000	5.6×10^{-2}	3256	3.86×10^{-2}	2247
50	1.92	1250	6.26	4070	4.32	2808
60	2.11	1500	6.86	4884	4.73	3370
70	2.28	1750	7.40	5698	5.11	3932
80	2.43	2000	7.92	6512	5.46	4493
90	2.58	2250	8.40	7326	5.80	5055
100	2.72	2500	8.85	8140	6.11	5616

* For $m=0$ deuterons at Enge set precessor field direction opposite to that in the inflection magnet.

Injection Beam Line Optics:

The injection beam line system starts with a three gap accelerating lens on the exit of the source deck. An einzel lens is used to focus the beam at the centre of the precessor. After the precessor, a second einzel lens is required to focus the beam through the inflection magnet onto the accelerator low energy Faraday cup. The precessor and the inflection magnets both have asymmetric focusing properties. To compensate for this, an electrostatic quadrupole lens was installed in front of each of these components. Detailed beam optics calculations have not yet been done. If the spin axis is precessed in the horizontal plane, the asymmetries of the precessor and the magnet add, and the beam tends toward a vertical shape at the injection focus. Because the two magnets are dipole devices, the quadrupole lenses do not properly compensate for this effect. This reduces the target beam intensity. When the spin axis is precessed in the vertical plane, the magnetic fields of the precessor and inflection magnets are perpendicular, and the asymmetries cancel in first order.

CHAPTER IV

CALIBRATION OF THE POLARIZED ION SOURCE

Before the start of experimentation using the polarized beam, a number of tests had to be run in order to establish operating parameters. These tests continued through the first period of experimental use. In order to optimize source output, the following parameters have been tested:

Neutral Beam Energy

Caesium Temperature

Argon Flow Rate

Krypton Adder Gas

Pure Vector Polarization

Precessor Calibration

Neutral Beam Energy:

As mentioned in the theory section, the optimum cross section for H(2S) production occurs at 500 eV for protons and 1000 eV for deuterons. However, ion optical effects must be considered. Higher neutral beam energies will improve the overall beam transmission. An empirical best current is likely to occur at a slightly higher value than that of the cross-section maximum. The beam was measured at the inflection magnet faraday cup. Results are displayed in figure 12. The best P^2I was at about 1.1 keV (for deuterons). This is in agreement with results from other laboratories.⁽²⁰⁾ One might have expected

that a secondary maximum would occur at about two kilovolts due to the H_2^+ beam. The absence of such a peak indicates that an unfavorable ratio of $H^+ : H_2^+$ can be detrimental.

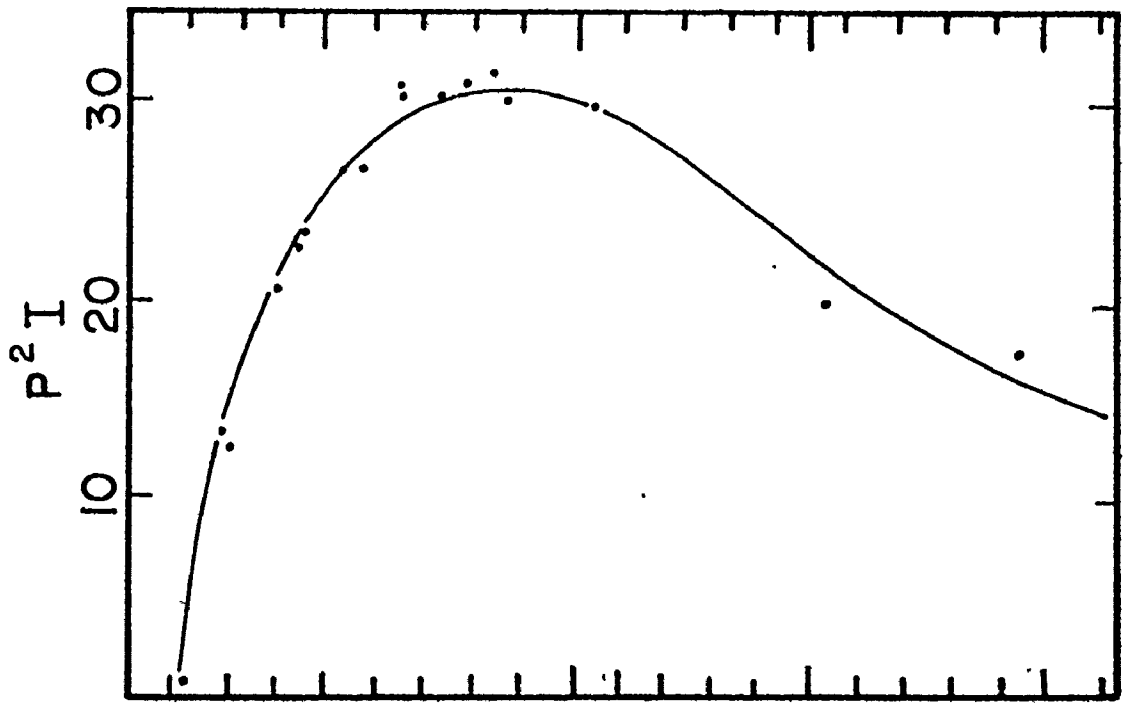
Caesium Temperature:

A large number of tests have been done on this parameter as we have had a lot of trouble with this unit. Three different reservoirs have been used. The first featured a valve stem that operated from the bottom of the reservoir up through the liquid caesium. Mechanical failures caused the abandonment of this design. A second design featured a valve stem operated from the back of the reservoir. This worked in a mechanical sense but the long passage between the reservoir and the canal was prone to blockage. The vapour pressure of caesium at these temperatures is about 5×10^{-4} torr. This is in the molecular flow region and a good conductance is therefore required between the canal and reservoir, that is, the connection between the canal and the reservoir should be open and short. The third design achieves this at the expense of remote operation of the valve. Maximum P^2_I occurs at about $100^\circ C$ for both the canal and the reservoir. Any deviation from this usually indicates some difficulty in the system. A sample set of measurements is presented in figure 10 shows the decrease in the value of "Q" at higher temperatures.

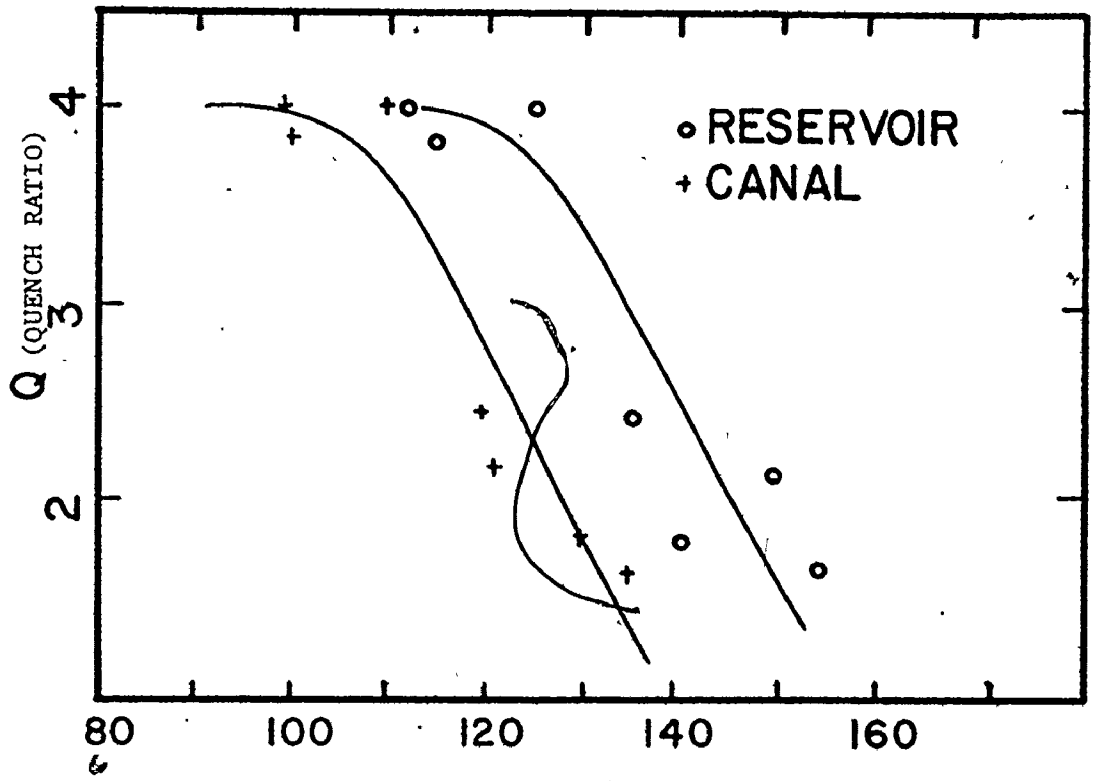
Argon Flow:

Repeated tests of this parameter failed to give reproducible results under all circumstances. The problem is that the important variable is pressure not flow. The equation:

$$\frac{Q(\text{Gas flow})}{S(\text{pumping speed})} = \text{Pressure}$$



ARGON FLOW (S.C.C.M.)



TEMPERATURE °C

FIGURE 10

governs the pressure. Pumping speed can vary greatly with the history of the cryopumps. When the pump surfaces are clean, their speed is quite high. After a number of days of running, there is a high enough vapour pressure from the pumping surfaces to maintain the exchange process. The data presented in figure 10 are typical of conditions in the first few days of operation. The usual best value is about one atmosphere ml. of argon per minute.

Krypton Adder Tests:

A paper was published by R.E. Olson et al⁽¹⁹⁾ in 1975 which suggested on a theoretical basis that krypton, not argon, would be the best adder gas. We therefore ran a test of this gas. The results displayed in figure 11a and b, suggest that this is not the case.

Argon Solenoid Setting for Pure Vector Polarization:

If the argon charge exchange of the $m_I = -1$ substate takes place in a field of about 9 gauss, the result should be pure vector polarization (see theory section). Using calibration points of magnet field vs current that were provided by the manufacturer, settings were selected for this test. These values were tested against experimental results using the reaction $^{12}\text{C}(d,\alpha)^{10}\text{B}$. For the 3.59 MeV 2^+ state, $T_{20} = 1/\sqrt{2}$ at 0° . This was used to detect the presence of any tensor polarized component in the beam. It was easily demonstrated that the value of T_{20} could be made to cross through zero. The user should be cautious when using this set up, as the value of T_{20} is critically dependent on the value of the magnetic field at the position where charge exchange occurs. This position is somewhat dependent on conditions in the argon canal region.

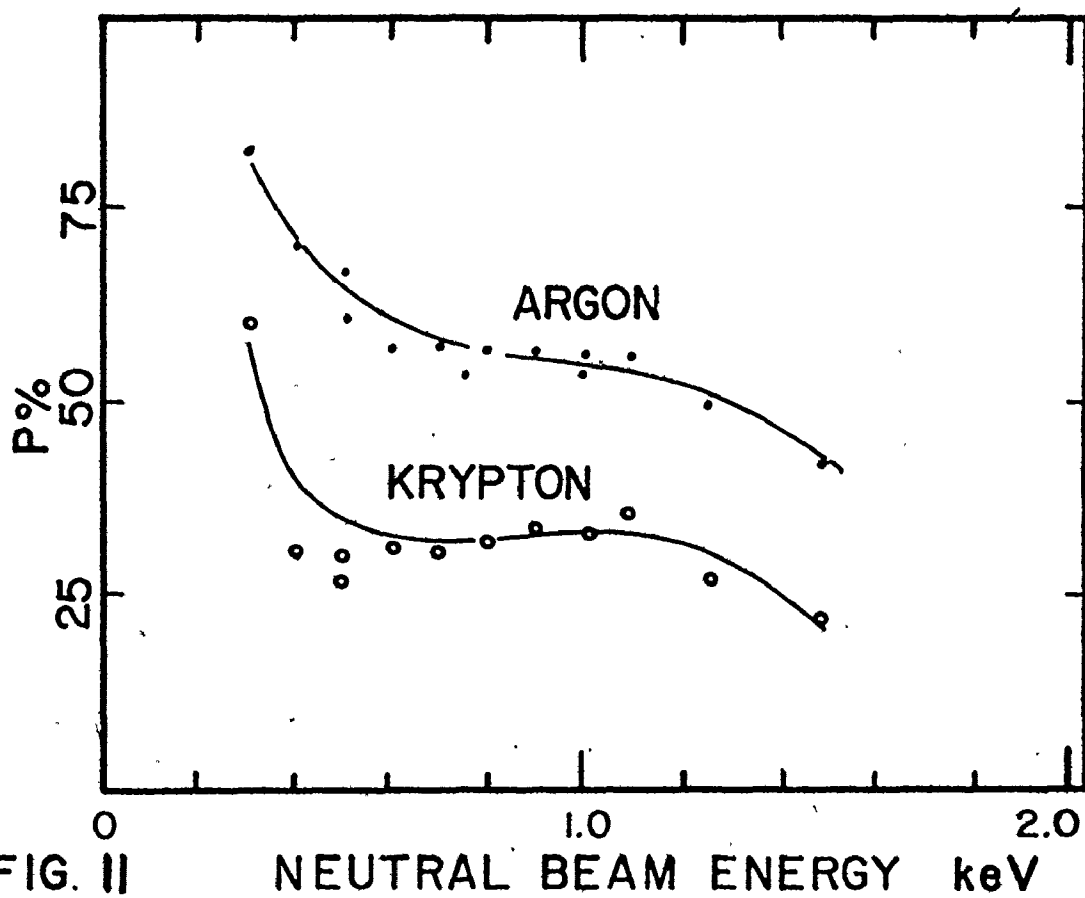
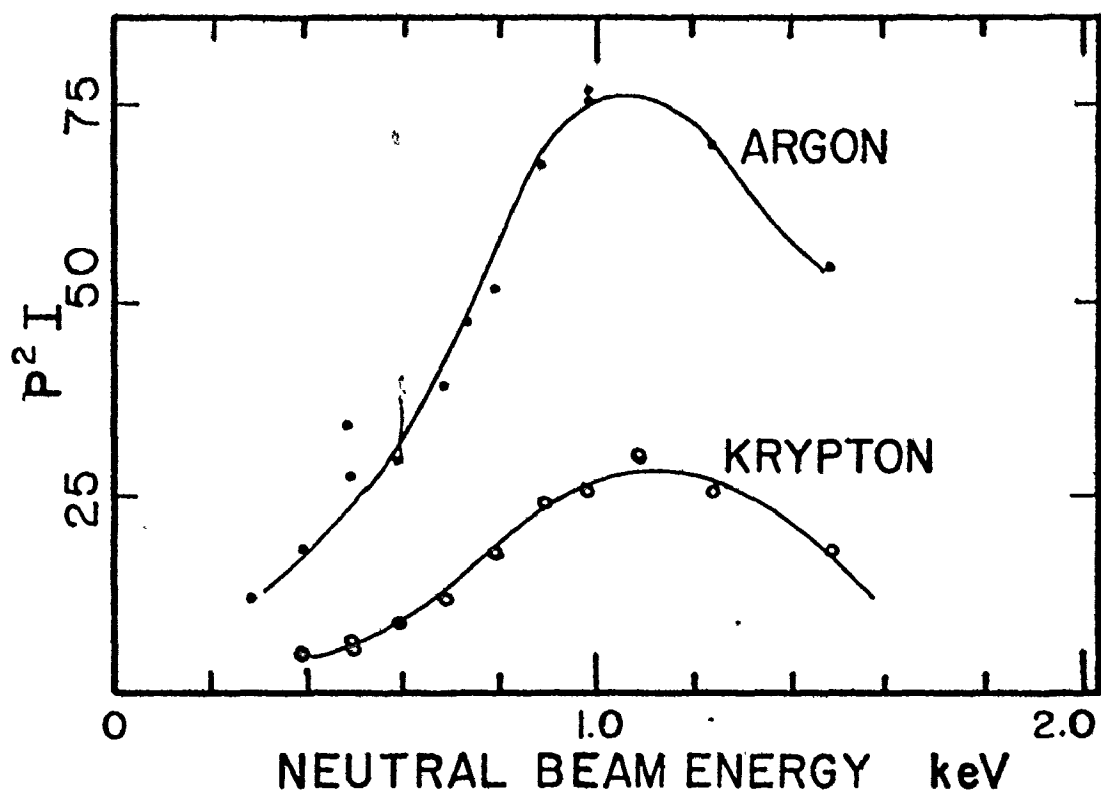


FIG. II

NEUTRAL BEAM ENERGY keV

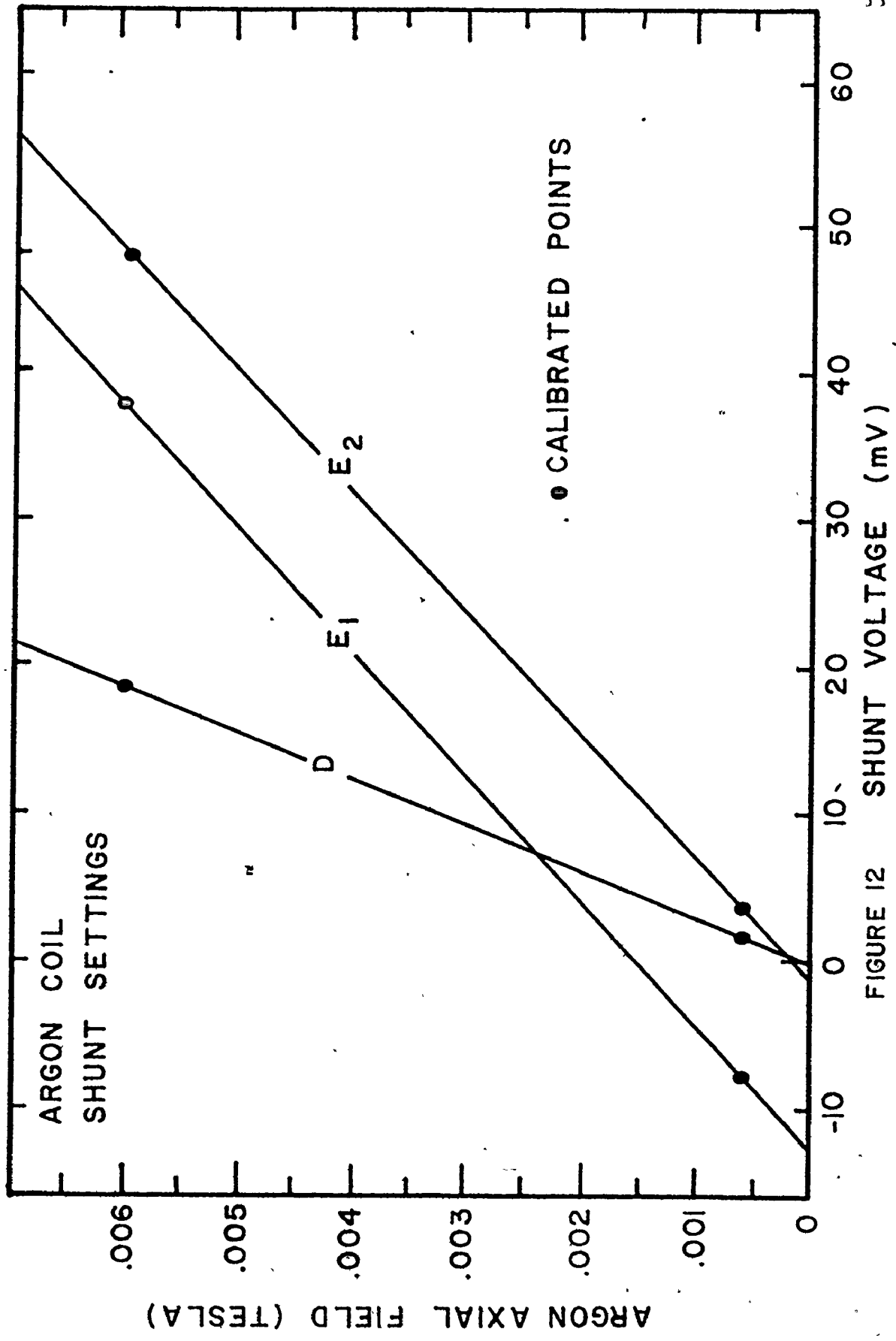


FIGURE 12 ARGON COIL SHUNT SETTINGS

Precessor Calibration:

The precessor was set according to the calculated values. This was tested by use of nuclear reactions. In many of our experiments there are internal calibration checks.⁽²⁾ Wherever possible these should be used to measure polarization rather than quench ratios. It is quite possible to get a quench ratio larger than the true value of polarization. In particular, incorrect setting of the precessor will not affect the quench ratio. An early set of data is displayed in figure 13, that was used to check the original calculations. Further checks have confirmed this calibration. It will be noticed that the variation is of a sine form and therefore small variations will not be of great importance until experiments are attempted that require polarization accuracies on the order of a fraction of a per cent.

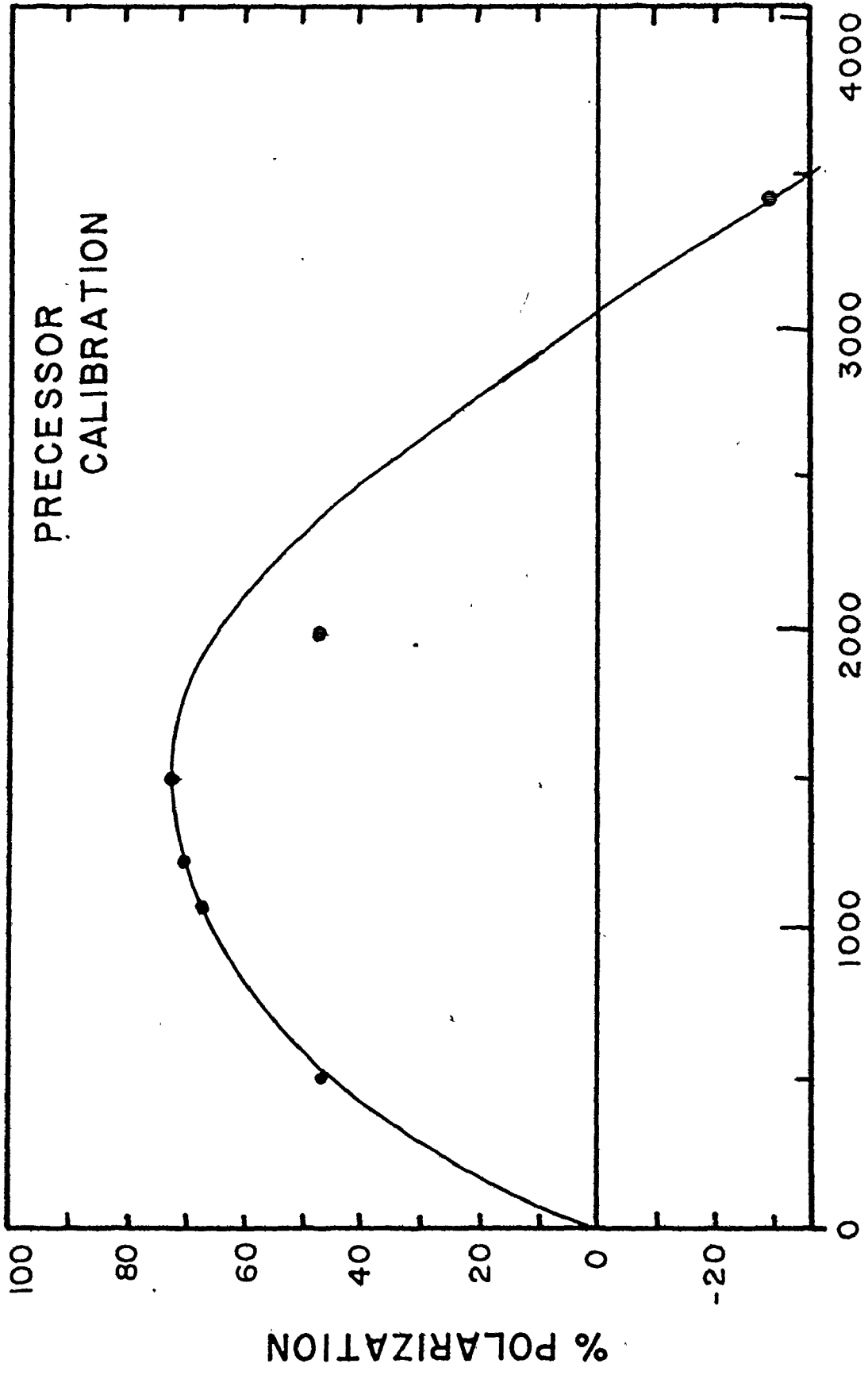


FIGURE 13. TOTAL PRECESSOR VOLTAGE

CHAPTER V

CONCLUSION

At the time this is being written, it has been about one year since the first polarized beam was accelerated at McMaster. The source has been scheduled for about 80 days of operation, or 20% of all F N operation. The process of calibration and development of the source has been intertwined with the experimental programme.

We have achieved a reasonable level of understanding of the source by now, and it is obvious that the interaction between nuclear physics research and the machine operation must be much closer in this type of experiment than might be the case in work involving more conventional beams.

There are many ways in which development of the source can continue. The injection optics problem can be pursued further. The internal construction of the device is such that real possibilities of shortening the path length of the low energy neutral beam can be envisaged. This would increase the total beam transmitted through the source but would increase the problem of deflecting the charged beam. Automation of the most used functions would greatly assist the experimenters. There are also surprising gaps in the knowledge of the source operation that should be pursued.

For example, the variation of the cross-section for the formation of negative ions in argon should be studied. Also, it is not apparent

that all of the beam produced by the duoplasmatron, is being used.

The completion of the modifications mentioned above and the pursuit of a more complete understanding of the source operation will be a continuing project of this laboratory in future years.

References

- 1) J. A. Kuehner et al, Phys. Rev. Lett. 35, 23 (1975).
- 2) G. D. Jones et al, Nucl. Instr. and Meth. 129, 527 (1975).
- 3) J. B. A. England, Techniques in Nuclear Structure Physics,
The Macmillan Press, London 1974, p. 612.
- 4) J. B. A. England, A Symposium on Polarized Beams, Daresbury
Laboratory, 10 January 1972, Proceedings, J. B. A. England ed. p.27.
- 5) H. F. Glavish, Proceedings of the Second Symposium on Ion Sources
and Formation of Ion Beams, Berkeley Calif. (1974) C. P. Pezzatti ed.
p. iv-1-1.
- 6) T. B. Clegg, Proceedings of the Symposium on Ion Sources and Forma-
tion of Ion Beams, Brookhaven Nat. Lab., Th. J. M. Sluyters ed.
(1971) p. 223.
- 7) P. G. Sona, Energia Nucleare 14, 295 (1967).
- 8) J. A. Kuehner et al, 4th International Symposium on Polarization
Phenomena in Nuclear Reactions, Zurich Switzerland, p. G46 (1975).
H. R. Weller et al, 4th International Symposium on Polarization
Phenomena in Nuclear Reactions, Zurich Switzerland, p. K9 (1975).
R. N. Boyd et al, 4th International Symposium on Polarization
Phenomena in Nuclear Reactions, Zurich Switzerland, p. G22 (1975).
R. N. Boyd et al, submitted to Phys. Rev. C
D. T. Petty et al, submitted to Phys. Rev. C
G. D. Jones et al, Phys. Lett. 59B, 236 (1975).
H. R. Weller et al, Phys. Rev. C. 13, 1055 (1976)
- 9) B. L. Donnally et al, Phys. Rev. Lett. 12, 502 (1964).

- 10) B. L. Donnally et al, Phys. Rev. Lett. 15, 439 (1965).
- 11) P. Pradel et al, Phys. Rev. A 10, 797 (1974).
- 12) J. L. McKibben et al, Phys. Rev. Lett. 20, 1180 (1968).
- 13) W. E. Lamb et al, Phys. Rev. 79, 549 (1950).
W. E. Lamb et al, Phys. Rev. 81, 222 (1951).
W. E. Lamb, Phys. Rev. 85, 261 (1952).
- 14) H. A. Bethe, Phys. Rev. 72, 339 (1947).
- 15) G. G. Ohlsen et al, Theory of a Radio-Frequency "Spin Filter" for a Metastable Hydrogen, Deuterium or Tritium Atomic Beam, Los Alamos Scientific Laboratory Report LA-3725 (1967).
- 16) J. L. McKibben, Proceedings of the Symposium on Ion Sources and Formation of Ion Beams, Brookhaven Nat. Lab., Th. Sluyters ed. (1971) p199
- 17) J. W. McKay, Proceedings of the Second Symposium on Ion Sources and Formation of Ion Beams, Berkeley Calif., C. P. Pezzatti ed. p. (N-4-1)(October 1974).
- 18) P. W. Keaton Jr. et al, Proceedings of the Third International Symposium on Polarization Phenomena in Nuclear Reactions, Madison Wisconsin, H. H. Barchall and W. Haeberli eds. p. 852 (1970).
- 19) R. E. Olson et al, Phys. Rev. A 13, 180 (1976).
- 20) T. B. Clegg, private communication.
- 21) T. A. Welton, Phys. Rev. 74, 1157 (1948)